

**1100 Seventeenth Street, N.W. Washington, D. C. 20036**

**FROM:** D. E. Cassidy

# BELLCOMM, INC.

SUBJECT: Some Considerations for the  
Atmospheric Entry of a Light  
Weight Manned Mars Landing  
Vehicle (MINIMEM) - Case 730

DATE: June 17, 1968

FROM: D. E. Cassidy

## MEMORANDUM FOR FILE

### 1.0 INTRODUCTION

The conceptual mission of the Mars Surface Sample Retriever (MSSR) probe<sup>1,2</sup> consists of performing the automatic (unmanned) functions of landing on the surface of Mars, recovering surface samples, launching from the surface, and completing a rendezvous with a manned flyby spacecraft sometime after the spacecraft passes periapsis. The high energy of the reference 1975 twilight flyby requires a total entry weight on the order of 11,000 pounds to ultimately return a 42 pound payload back to the manned flyby spacecraft. A 60° blunted cone entry vehicle configuration with a 20 foot base diameter would deliver the 4000 pound ascent stage (surface launch vehicle) through a ballistic entry trajectory to the Martian surface.

Due to the relatively high energy at Mars for the twilight flyby missions, (approximately 36,000 fps ascent  $\Delta V$  required to rendezvous in 1975, and higher in later years) a substantial increase in ascent payload is possible for rendezvous within an elliptical parking orbit during the stopover missions. It was shown in reference (3), that a vehicle weighing 15,000 pounds at initial atmospheric entry has the potential of returning on the order of 900 pounds of payload from the surface of Mars to a spacecraft in a highly elliptical orbit. With relatively large payload capability, it is reasonable to consider the possibility of including a man as part of the payload. As a development goal, then, the precursor unmanned MSSR would perform unmanned surface sample recovery in support of the early manned flyby missions while inherently providing much of the testing, qualifications, and confidence required for ultimately man-rating the system for later stopover/landing missions.

The ability to package a man in such a minimum weight system is discussed in reference 4. Within the ground rules specified, a one-man ascent capsule would weigh just over 700 pounds and a two-man capsule on the order of 1,300 pounds. These weights would grow to atmospheric entry weights on the order of 15,000 pounds for the one-man vehicle and 35,000 pounds for the two-man vehicle with a surface shelter integrated within the landing stage. As a possible option, the manned vehicles could be supported on the Martian surface with unmanned logistics vehicles

for extended mission capability as well as mission flexibility. If such a scheme was selected, it would then be most desirable for the unmanned logistics vehicles to be as identical as possible in entry and landing systems to the manned vehicles (MINI-MEM) in order to complement the overall probe development program.

## 2.0 STUDY SCOPE AND ASSUMPTIONS

The purpose of this memorandum is to investigate some of the operational aspects of a manned Mars landing mission and to compare various trade-off parameters. Primary emphasis will be placed on the following considerations:

1. Out-of-orbit ballistic (non-lifting) entry vs. lifting entry,
2. Out-of-orbit lifting entry vs. hyperbolic lifting entry, i.e., direct from the hyperbolic approach trajectory,
3. Entry guidance and control requirements,
4. Landing site targeting and surface rendezvous capability,
5. Effect of lift-to-drag ratio ( $L/D$ ) and ballistic parameter ( $m/C_D A$ ),
6. Mission abort opportunities, and
7. Terminal landing.

The direct entry analysis will center on an entry velocity of 25,000 fps ( $V_\infty = .2$  emos). This represents a reasonable upper limit for the approach velocities associated with stopover missions. The out-of-orbit entry will be from a highly elliptical (24 hours) orbit with a resulting entry velocity on the order of 15,500 fps. Entry altitude is defined at 700,000 feet.

It is assumed that prior to the manned stopover missions, considerably more will be known about the Mars environment to provide substantially more confidence in the structure of the atmosphere. Since the VM-8 atmosphere essentially presents the worst entry conditions,<sup>1</sup> except for the terminal landing phase, it is assumed in this study, that the VM-8 atmosphere describes the nominal density profile.

In addition, a capsule type entry vehicle similar to the MSSR vehicle will be used in the analysis<sup>1,2</sup>. Both the Apollo shape and a 60° cone will be considered as optional configurations.

### 3.0 AERODYNAMIC CHARACTERISTICS AND CONFIGURATIONS

The vehicle configurations are shown in Figure (1), and the corresponding static aerodynamic performance parameters are presented in Figures (2) and (3)\*. The ballistic parameters in Figure (2) correspond to various gross weight vehicles with a 20 foot maximum diameter, while the effects of reducing the diameter on a 15,000 pound gross weight vehicle are presented in Figure (3). Both configurations are in the same L/D category, but at a given L/D, the Apollo shape has a lower ballistic parameter and lower trim angle-of-attack\*\*.

The ranges of ballistic parameter and L/D which will be investigated are indicated by the darkened circles on Figure (3). The upper values will define the "heavy" vehicle and the lower values the "light" vehicle\*\*\*. The ballistic parameters for the non-lifting case corresponds to  $L/D = 0$ .

### 4.0 BALLISTIC ENTRY ( $L/D = 0$ )

In this section, the MSSR configuration as outlined in references (1) and (2) is investigated for use as a manned vehicle. In the case of the unmanned MSSR mission (32,000 fps entry velocity), no lifting capability was provided since there was no clear requirement to employ lift at the time when the studies were conducted.

---

\*Whether it is reasonable to package these vehicles with sufficient c.g. offset to provide the required trim for the high L/D's is not considered here. For this reason, lower values of L/D (i.e., lower angle-of-attack) are used in the study than are theoretically obtainable from the configurations.

\*\*It is desirable to maintain a low angle-of-attack to minimize c.g. offset and to permit a larger packagable volume behind the forward heat shield, Figure (1).

\*\*\*The heavy vehicle is essentially two-man and the light vehicle is one-man<sup>4</sup>. The choice of curves on Figure (2) was made to establish the limits for the parametric study which follows and not to specify a configuration.

The G loads\* are sufficiently low for unmanned systems (40 G), the entry corridor appears achievable (10 n.m.), and the landing propulsion requirements are reasonable (approximately 3000 fps). A manned entry vehicle, on the other hand, requires some additional considerations including the maximum G loading on the crew.

It was pointed out in reference (3), that entry could be performed ballistically from an elliptical orbit without exceeding 10 G's, but probably not directly from a hyperbolic approach trajectory because of the very small entry corridor. The main difficulties with the manned ballistic entry from an elliptic orbit, however, are associated with the large landing site uncertainties that result from shallow entry angles required for low G entry, and the inability to make range corrections without lift vector control. In addition, the extra weight of the manned vehicles, particularly the two-man version can make the terminal propulsion maneuver for the ballistic entry very expensive as compared with the unmanned MSSR.

Parameter sensitivities for ballistic entry from a 24 hour elliptical orbit are summarized in Figures (4) and (5). As in reference (1), the velocity at 20,000 feet altitude is representative of the required terminal propulsive ( $\Delta V$ ) maneuver for a soft touchdown without any additional provisions for hover and site selection time. The numerical differences between the "Approach Trajectory Periapsis Altitudes" in Figures (4) and (5) define the entry corridor widths, and the numerical differences between the "Down Range from Entry" represent the landing point uncertainty resulting from the entry corridor width.

The MSSR entry system (with a 20 foot base diameter) configured as a one-man vehicle similar to reference (4) would have a ballistic parameter of about  $1.0 \text{ slug/ft}^2$  at a gross entry weight of 15,000 pounds. For a maximum deceleration limit of 10 G's, the terminal propulsion  $\Delta V$  required for a soft touchdown would be on the order of 3500 fps, referring to figure (4). This compares with about 3000 fps for the unmanned MSSR ( $m/C_D A = .8 \text{ slugs/ft}^2$ ). The corresponding accuracy to which the landing site can be predicted depends on the accuracy to which the approach guidance can determine the proper approach conic, and thereby achieve the entry corridor. For a five nautical mile corridor (a five nautical mile difference in periapsis altitude of the approach conic), which should be a reasonable estimate when operating from an elliptical orbit (ten nautical miles was assumed for direct entry

---

\*G refers to the acceleration in units of earth sea level acceleration of gravity ( $32.2 \text{ fps}^2$ ).

at 32,000 fps)<sup>1</sup>, the landing point error could be as much as thirty nautical miles ( $\pm 15$ ) on the surface, Figure (6). A two nautical mile corridor, on the other hand, results in about a ten nautical mile maximum surface error\*. Since the landing site uncertainties are based on a 10 G undershoot, if the maximum deceleration limit is reduced to 8 or 6 G's a substantial increase in the landing uncertainties would result from the shallower entry angles.

For a two-man version<sup>4</sup> (35,000 pounds) the ballistic parameter would be between 1.0 and 2.5 slugs/ft<sup>2</sup> for base diameters of 30 feet and 20 feet, respectively. It is apparent from Figures (4) and (5), that the larger ballistic parameter can be extremely expensive in terminal propulsion, and will shift the entry corridor to shallow trajectories (large periapsis altitudes, low G entry) which have associated with them larger landing site uncertainties. A 30 foot diameter two-man vehicle, on the other hand, would have characteristics similar to the 20 foot one-man ( $m/C_D A \approx 1$ ).

As a summary, then, it is feasible to enter a manned capsule without lift from a highly eccentric Mars orbit. However, the landing propulsion is very sensitive to ballistic parameter, narrow entry corridors are required, and large landing point uncertainties are inherent. Therefore, the concept of utilizing the ballistic vehicle for a manned, as well as unmanned, is probably not desirable. A preferable approach to MSSR & MINIMEM commonality would be to configure the unmanned MSSR for lift and provide either a controlled entry or fixed lifting entry for the higher energy flyby missions. This scheme will require additional analysis. The work that follows considers the manned lifting entry case and the factors influencing its design.

## 5.0 LIFTING ENTRY

Both the direct and the out-of-orbit entries are analyzed in this study with the same basic entry and landing modes. The vehicle is guided to an initial entry corridor with the aerodynamic

---

\*It is not clear how accurately probes could be targeted from Mars orbit. It is expected, however, that orbital targeting will be inferior to the accuracies achievable with earth based tracking of out-of-earth orbit entry vehicles. The last two Mercury (ballistic) flights MA-8 and MA-9 for example, achieved landing site miss distances of 5 and 4.5 nautical miles. respectively. The last five Gemini (lifting vehicle) flights were all within 2.7 nautical miles.

lift vector directed up (positive lift)\*. In the neighborhood of pullout ( $\gamma \approx 0$ ), the lift vector is modulated to hold a constant altitude by rolling the vehicle around the velocity vector at a constant angle of attack. The ballistic parameter is thereby held constant while the velocity is reduced sufficiently to secure capture. The constant altitude phase is followed by terminal ranging and propulsive descent for a soft touchdown on the Martian surface. Small range errors can be corrected with the landing propulsion system, but such a scheme becomes very expensive in propellant consumption for range errors larger than a mile or so, as will be shown later. It is desirable, then, to null all range errors while still decelerating aerodynamically.

In this study, only the cases where the landing site is in the entry plane are considered so that no lateral ranging is required. However, in terms of implementing cross-range error compensation, it is arbitrary for pitch plane maneuvers whether the vehicle is rolled toward the right or left. In the course of entry maneuver, then, the integrated lateral accelerations (proportional to  $V^2$ ) would be directed the same toward the left and right cancelling any lateral range bias. This averaging technique could be accomplished by a rocking motion or complete  $360^\circ$  rolls. The cross-range errors are primarily a function of on-board sensor accuracies, however, and will require more detailed analysis than is intended here.

## 5.1 Entry Corridor Definition for Lifting Entry

### 5.1.1 Overshoot

The shallowest entry angle (highest vacuum periapsis altitude) at which the vehicle can enter is determined by the minimum altitude to which it penetrates following entry. If sufficiently low altitude is not reached (i.e., high enough atmospheric density), the lift force generated with full lift down after pullout will not balance the centrifugal force and the altitude cannot be held constant. The altitude where lift just balances centrifugal force, neglecting the effects of gravity, is defined as the maximum allowable pullout altitude ( $H_m$ ) for this study. This altitude will be used to define the overshoot.

---

\*Negative lift can be used on the overshoot to reduce down range dispersions. It is also possible to define the overshoot limit with negative lift which can have the effect of widening the entry corridor. This is discussed later in the paper.

$H_m$  is a function of the atmospheric density and the lifting parameter ( $m/C_L A$ ) of the vehicle. Values of  $H_m$  are presented in Figure (7) for the VM-8 atmosphere with the shaded region corresponding to the entry vehicle characteristics outlined in Figure (2).

The inclusion of the gravity force would permit higher pullout altitudes since gravity acts in the direction opposite to the centrifugal force, so that the pullout altitude could be extended to near the equilibrium glide boundary, Figure (8). The use of  $H_m$  however does represent a degree of conservatism. Entry near the equilibrium glide boundary results in high heating loads, and large range error sensitivities due to corridor and atmospheric uncertainties. The differences between  $H_m$  (Figure 7) and the equilibrium glide altitudes are presented in Figure (9). It is noted that the differences depend only on velocity and become less at high velocities where gravity has less effect. At 25,000 feet per second, the difference is about 4,500 feet of altitude, or approximately 25% of the VM-8 atmospheric scale height. Although the difference becomes as much as 15,000 feet of altitudes at 15,500 feet per second, corresponding to the out-of-orbit case, it will be shown later that the out-of-orbit entry will not be influenced by  $H_m$  since the wide corridor available makes it unnecessary to approach the overshoot limit.

#### 5.1.2 Undershoot

Since the Martian atmosphere is characterized by low densities, it is important to maintain sufficiently high pullout altitudes to insure that high surface protuberances can be cleared during entry. This is of particular concern for vehicles with high values of ballistic parameter, and could restrict the steepest entry angles. For the relatively small values in ballistic parameter corresponding to the MINIMEM configurations, however, the steepest entry angle is determined primarily by the maximum deceleration loads imposed on the crew and structure and will probably not be influenced appreciably by pullout altitude.

The maximum deceleration loads experienced during entry depend on the atmospheric density profile and the ballistic parameter, but only weakly on  $L/D$  (for  $L/D \leq .5$ ). The altitude-velocity deceleration load lines for the VM-8 atmosphere are presented in Figure (10) for constant values of the parameter  $G \cdot m/C_D A$ , i.e., product of deceleration times ballistic parameter ( $\text{slugs/ft}^2$ ). The load lines are valid for lift-to-drag ratios ( $L/D$ ) up to .5.

The maximum pullout altitudes in Figure (7) and the load limit lines in Figure (10) represent the boundaries within which the manned Mars entry vehicle will operate. The ability to remain



within these boundaries depends on the accuracy of the initial entry corridor, knowledge of position in the corridor and the execution of the required control, i.e., roll attitude commands. The differences in vacuum periapsis altitude between the shallowest entry angle and the steepest entry angle define the entry corridor width.

## 5.2 Direct Entry From Approach Hyperbola

### 5.2.1 Entry Corridor Requirements

For a maximum deceleration limit of 10 G's, the ideal entry corridor\* for direct entry into the VM-8 atmosphere at 25,000 fps from an approach hyperbolic trajectory is presented in Figure (11) as a function of ballistic parameter. The corridor specifies the accuracy requirements in the approach trajectory periapsis altitude (or entry angle) in order to hold decelerations less than 10 G and still maintain a controlled constant altitude entry.

It is of interest to note that for a given L/D, there is a value of  $m/C_D A$  where the corridor width is a minimum; the corridor does not monotonically decrease with increasing ballistic parameter as would be the case with an adiabatic atmosphere. This phenomenon is a direct result of a tropopause (separation of adiabatic and isothermal regions), at 61,000 feet altitude for the VM-8 atmosphere, below which the density gradient is more gradual (higher effective scale height). Consequently, the peak decelerations are lower if the ballistic parameter is high enough so that pullout occurs below the tropopause altitude.\*\*

The minimum pullout altitudes, corresponding to the under-shoot (10 G) trajectories, are also indicated in Figure (11). A minimum altitude of 40,000 feet is suggested to provide sufficient contingency for terrain clearance and atmospheric variations. The shaded portion of Figure (11) covers the aerodynamic parameters outlined in Figure (2) and represent the range in values for the light and heavy vehicles. This shows that for a given L/D, the lower ballistic parameter (light) vehicle has a smaller entry corridor, but the heavier vehicle will pullout at lower altitudes.

The influence of lift-to-drag ratio on entry corridor and maximum decelerations for the light and heavy vehicles are presented in Figure (12). In order to meet a 10 nautical mile entry corridor and not exceed 10 G's, an L/D of approximately .4 is required for the

---

\*Assuming the Mars atmosphere has exactly the VM-8 profile and the vehicle aerodynamics are known precisely.

\*\*The statement applies to the VM-8 atmosphere due to the low density profile.

lighter vehicle and .35 for the heavier vehicle. Since the capsule configurations have maximum L/D's of .45 to .5, a 10 nautical mile corridor will not permit reductions in the undershoot limit to less than about 9 G for direct entry at 25,000 fps. With improved entry guidance, however, entry can be made shallower and the peak decelerations can be reduced.

### 5.2.2 Landing Point Control Requirements

The problem of landing site selection or surface rendezvous involves the ability to reach a pre-selected landing site regardless of where in the corridor entry takes place. It is assumed here that all positions in the corridor are equally likely. Entry near the overshoot requires roll control to reduce the range (impossible if initial entry was made with full lift down near the equilibrium glide), and entry near the undershoot requires roll control to increase range.

The down range landing point uncertainty resulting from a 10 n.m. entry corridor width is presented in Figure (13) for the light vehicle with L/D's from .25 to .45, and the heavy vehicle for an L/D = .36. In the case of the light vehicle with L/D = .36, a 10 n.m. entry corridor results in a possible landing point location anywhere between 950 nautical miles and 1,600 nautical miles from the entry point if no range control is employed. This 650 nautical mile uncertainty results from a pre-programmed constant altitude entry. In mission planning, the target landing point would be placed somewhere within the dispersion, say around the mean (1,275 nautical miles), and then the guidance and control capability must be provided to remove the  $\pm 325$  nautical mile potential error in order to reach the landing point from either of the two edges of the corridor ( $\gamma = -16.7^\circ$  to  $-17.4^\circ$ ). The ability to reduce such a large dispersion is dependent on how accurately the position within the corridor is known at entry and the amount of lift control that can be used to modulate the entry trajectory.

#### Control From Pullout

If entry occurs near the undershoot, the range can be gained by delaying the roll maneuver (i.e., maintaining lift up) until sometime past the pullout. The effects of applying this maneuver to the light vehicle is illustrated in Figure (14) for a  $20^\circ/\text{sec}$  roll rate\*. For entry right at the undershoot ( $-17.4^\circ$ ), a delay of about 6.5 seconds past pullout would permit the required gain in range. It is obvious, however, that this maneuver is quite sensitive since small increases in the delay time and small uncertainties in corridor position produce large variations in range.

---

\*Following a simplified control law using a constant magnitude of roll rate and the sign of the flight path angle to specify the direction of roll.

Reducing the range when entering near the overshoot can be accomplished with negative lift. The effect of this maneuver is illustrated in Figure (15). If the position in the corridor is near the overshoot ( $-16.7^\circ$ ), the lift vector is rolled negative until a preset deceleration threshold is reached and then the lift is again rolled positive. The maximum decelerations experienced during this maneuver are included in Figure (15)\*. For entry right at the overshoot, GM would be set equal to 2 and approximately 7 G's would result from reducing the range to the nominal value. Small errors in the position, however, can cause over-correction and high decelerations, as illustrated in Figure (15).

For surface range control, therefore, the overshoot as well as the undershoot can result in high decelerations.

#### Control After Blackout

From atmospheric entry down to some sufficiently low velocity, trajectory control would be based essentially on inertial navigation and initial conditions data. At some point in the trajectory, however, the vehicle would exit from "blackout" and additional state data could be obtained from doppler signals, radar altimeter, ground beacon, etc. This surface tracking data could then be used as a basis for initiating range control. An indication of the maximum range control capability from this point was obtained by assuming that control is initiated at a velocity of 10,000 fps. The maximum range control using full +L/D and full - L/D is presented in Figure (16) for different initiation altitudes. Also included in Figure (16) are the traces of pullout altitudes and ranges-to-go resulting from the 10 nautical mile entry corridor. In addition, the maximum line-of-site ranges corresponding to the given altitude are indicated.

Although on the order of 200 miles of down range can be gained at this point, the landing site would not be visible at the time of control initiation. This would be most significant if it is desired to employ a homing beacon on the surface as might be the case for surface rendezvous. For terminal beacon homing, therefore, the maximum range control will probably be governed by the line-of-site limit and not by the vehicle aerodynamic performance capability.

---

\*The same control law was employed as in the case of the undershoot. In addition, roll from negative to positive was initiated when a specified deceleration limit (GM) was reached. Depending on the limit value, the roll is delayed resulting in reduced range and increased maximum deceleration.

Even without such a constraint, control from this point on the trajectory is not sufficient to eliminate the range errors resulting from an entry corridor 10 nautical miles wide. This is illustrated in Figure (17) with the light vehicle. The solid line is the trace of the landing points for the nominal entry corridor and the dashed lines are the result of employing the maximum positive lift to increase range or maximum negative lift to decrease range as previously discussed. It can be seen that a residual landing point error of as much as 100 nautical miles (+50) for the light vehicle (correspondingly, it is approximately 150 nautical miles (+75) for the heavy vehicle) results from control at this point in the trajectory if no previous corrections were made within the entry corridor. Control must therefore be initiated early during the pullout phase to eliminate all range errors resulting from the 10 nautical mile corridor.

With more accurate entry guidance, however, the entry corridor can be reduced and it would then be possible to eliminate the range errors at this later point in the trajectory. For an entry corridor less than about 8 nautical miles, maximum control just after blackout will result in no residual errors. Of course, the question of whether sufficient data would be accumulated so that control could actually be initiated at a velocity of 10,000 fps will have to be answered. A corridor capability somewhat less than 8 nautical miles would probably be more realistic.

On the other hand, if an entry corridor 10 nautical miles wide is determined to be too narrow for approach guidance at Mars, or if a larger margin of safety is desired, then it will be necessary to either increase the maximum deceleration limit, employ a higher L/D entry vehicle configuration, or utilize negative L/D to widen the entry corridor. The first two items will not be investigated in this study, but the use of negative L/D overshoot will be considered.

### 5.2.3 Negative Lift Overshoot

Employing negative lift prior to entry permits entry at shallower angles and can result in widening the entry corridor. This is illustrated in Figure (18). For the light vehicle with an  $L/D = .36$ , the overshoot can theoretically be extended from  $-16.7^\circ$  to just under  $-16.2^\circ$ . The ability to use all this additional  $.5^\circ$  (6 n.m.), however, depends on the strategy employed to keep the peak decelerations below the allowable maximum.

Since the vehicle would be entering with negative lift, it must at some point be rolled positively to prevent "dive-in". The data in Figure (18) are based on a strategy whereby the vehicle is rolled toward positive L/D when the G level reaches a given

value, GM, and then maximum positive L/D is held until pullout ( $\gamma=0$ ). The maximum deceleration experienced during the maneuver depends on the value of GM and the entry angle. A larger value of GM delays the roll maneuver and permits deeper penetration into the atmosphere. The positive L/D boundary (from Figure 13) represents the condition where the lift is initially positive or rolled positive under a very low GM signal.

It can be seen from Figure (18) that one way to widen the entry corridor would be to set a large GM for shallow entry angles and small GM for steep entry angles. The problem with this approach, however, is that unless there is an accurate knowledge of the position within the corridor, a small preselected value of GM would have to be used in all cases and no net gain in usable corridor is obtained. This can be seen with an example. If GM is always set equal to 3, the vehicle could enter between  $\gamma = -16.15^\circ$  and  $\gamma = -16.9^\circ$  and not exceed a 10 G undershoot. This, however, represents no improvement over the +L/D corridor width and has the disadvantage of a larger range dispersion. Therefore, accurate knowledge of position within the corridor is necessary in order to take advantage of the wider negative L/D corridor by selecting GM according to position.

### 5.3 Out-Of-Orbit Entry

#### 5.3.1 Entry Corridor Requirements

Since the entry velocity is considerably lower from out-of-orbit, the deceleration loads at a given entry angle are much lower than the direct entry case and a tighter control on the landing point is possible while still maintaining both acceptable G loads and pullout altitudes.

In Figure (19), the corridor width requirements based on a 5 G undershoot\* are presented for a range in L/D and  $m/C_D A$ . The overshoot is defined here by the maximum altitudes,  $H_m$ , of Figure (7), which are independent of entry velocity and were also used in the direct entry case. It is obvious that the corridor is substantially wider than it was for the direct entry (Figure 13) and that substantially lower G's can be maintained.

In Figure (20), the influence of maximum deceleration and L/D on corridor width for the heavy and light vehicles is also presented. Here, it can be seen that it is possible to enter at less than 4 G with a 10 nautical mile corridor and under 3 G for a 5 nautical mile corridor.

---

\*5 G undershoot was chosen for illustrative purposes since 10G provides corridors which are larger than is apparently necessary.

Alternately, the range dispersion can be reduced appreciably for a given corridor width by shifting the corridor to steeper entry angles and higher G's.

### 5.3.2 Landing Point Control

The range sensitivities to entry angle are illustrated in Figure (21) for both the light and heavy vehicles. A 5 nautical mile corridor, defined between entry angles corresponding to approximately 4 G and 5 G, would result in a landing point uncertainty of about  $\pm 35$  nautical miles. Reducing the peak deceleration limits to between 3 G and 4 G would increase the landing point uncertainty to about  $\pm 50$  nautical miles. This  $\pm 35$  to  $\pm 50$  nautical mile error could easily be corrected after the vehicle velocity has reduced to below 10,000 fps as illustrated in Figure (16), indicating that initiation of range control can be delayed until additional state data becomes available after the end of blackout as discussed previously.

In terms of entry corridor, deceleration loads and landing site control, the out-of-orbit entry provides advantages over the direct mode. The permissible entry corridor is much wider, and pre-entry targeting is most likely better than in the direct mode so that narrower entry corridors can be used (additional study is required for a quantitative comparison). As a consequence, the peak decelerations can be held to 4 G or less, and range control is probably not required until after the end of blackout.

## 6.0 AERODYNAMIC HEATING AND WEIGHT PENALTIES

### 6.1 MSSR/MINIMEM Comparison

The direct and out-of-orbit entry modes are compared in Figure (22) for the unit area convective heating load in the stagnation region as well as the trajectory time from entry to the surface. The heating load reflects the heat shield ablator material requirements and the entry time represents the thermal heat soak period which effects the insulation requirements--the insulation weight including non-pyrolyzing ablator material is approximately proportional to the square root of the heating time, for similar material thermal properties. The heating rates were computed for a blunt configuration using the corrections for angle-of-attack of the Apollo vehicle suggested in reference (5). The resulting effective nose radius used in the calculation was 4 feet for the 20 foot diameter Apollo type configuration.

The stagnation heating loads for the heavy and light MINIMEM vehicles are compared with those on the earth entry Apollo suborbital flight AS-202 as well as those estimated for the non-lifting unmanned MSSR.<sup>1</sup> Although the heating load in the stagnation region for the unmanned MSSR (at 32,000 fps) is primarily from convective transport, the maximum diameter regions experience large radiation heating. It is estimated that the radiation heating on the MSSR could be about 50% of the convective heating when integrated over the whole surface. On the other hand, due to the lower velocities and higher angle-of-attack, the MINIMEM receives practically all of its heat load through convection. In comparison with the unmanned MSSR,<sup>1</sup> then, the heating distribution and form of heating will be different for the MINIMEM, and the heating time will be longer by as much as a factor of 4. In addition, the peak deceleration load for the MSSR is on the order of 40 G's compared to a 10 G limit for the MINIMEM. It is concluding, therefore, that the entry environment for the MSSR and MINIMEM can be substantially different dictating different heat protection and structural requirements.

At least two approaches that could be taken to make the two systems similar would be to design to the higher structural loads of the MSSR and the longer heating period of the MINIMEM, or to configure the unmanned MSSR with lift and maintain the entry environment similar to the MINIMEM. The degree of commonality that is actually desired will dictate the approach that should be taken. More detailed study is required to determine the weight and systems tradeoffs.

## 6.2 Entry System Weight Estimate

An upper bound to the entry heat protection and structural weights of the MINIMEM were obtained from a comparison with the 3-man Apollo vehicle (CM) used in the AS-202 sub-orbital test mission. The AS-202 entry velocity was on the order of 28,000 fps. It is noted in Figure (22) that the thermal load and heating times are less for the MINIMEM for direct entry, compared to the AS-202 mission, and substantially less in the case of the out-of-orbit entry. It is also noted that the thermal load from a lunar return mission can be from 2 to 2 1/2 times the AS-202 mission thermal load, so that the Apollo (CM) actually represents an overly conservative design base and should certainly represent an upper bound. The Apollo (CM) thermal weight penalty (ablator, insulator and structure outside of the pressure shell) represents about 15% of the vehicle gross weight. Since the ballistic parameter of the heavy weight MINIMEM vehicle is similar to the Apollo (CM), it would appear that a 10 to 15% weight

penalty would be an upper bound for the two man MINIMEM.\* This compares with a recent North American Rockwell study<sup>6</sup> which estimated about 12 to 13 percent for their 82,000 pound, 30 foot diameter, 2-man/4 day MEM vehicle with a ballistic parameter similar to the heavy MINIMEM.

In the case of the light weight MINIMEM, however, a larger percentage weight penalty is incurred due to the lower ballistic parameter and therefore larger wetted area to gross weight ratio. An estimate of the thermal weight penalty for the light vehicle is obtained by multiplying the ratio of ballistic parameters times the 10 to 15%, resulting in 27 to 40 percent. The lower limit is probably more realistic in light of the conservative design base. Coincidentally, 30% is approximately the weight penalty for the MSSR,<sup>1</sup> although as discussed previously, the distribution of weight between structure, ablator and insulation would be different.

It is felt that the 10 to 15 percent for the heavy vehicle and 30 percent for the light vehicle are quite conservative since the entry systems weight might be reduced substantially with the use of improved ablator materials and lower design entry G's. The AVCOAT 5026-39 ablation material used on the Apollo (CM) and the North American Rockwell MEM<sup>6</sup> have a virgin bulk density of about 31 pounds/ft.<sup>3</sup> and thermal conductivity of .61. Superlight ablator materials (SLA) currently under investigation have densities and thermal conductivities on the order of 1/2 the AVCOAT material.<sup>7</sup> Since SLA materials are presently considered for lower surface shear applications (low dynamic pressures), they would probably find more direct application in the low G out-of-orbit entry. However, composite forming of the SLA materials with other high density and high shear materials could provide for the higher G entries and also result in lower total weight.

## 7.0 ADDITIONAL CONSIDERATIONS

### 7.1 Mission Abort

Manned entry into Mars introduces the question of mission abort opportunities and constraints. A schematic representation of abort modes during various phases of Mars entry is

---

\*For the same  $C_D$ , the ballistic parameter ratio in effect compares the vehicle wetted area to the gross weight. Since the type of heat protection and structure involved here is essentially surface area dependent, the wetted area to gross weight ratio is approximately proportional to the weight penalty.



presented in Figure (23). Before the entry vehicle engages the atmosphere, the propulsive landing stage could be fired to deflect the approach conic. It will be assumed that this maneuver must be initiated well before the nominal entry point to prevent significant aerodynamic heating. The reason for this is that engine is designed to accommodate high heating rates while in operation, but not while shut-down. In addition, sequencing the engine exposure and engine start could introduce operational problems.

For direct entry at 25,000 fps, it is shown in Figure (24) that an abort can be initiated without onset of significant heating down to about 200 seconds before the nominal entry in the VM-7 atmosphere, and just under 100 seconds before entry in the VM-8 atmosphere. This assumes a thrust to earth weight ratio of 1.0 and a propulsive  $\Delta V$  of 3,000 fps, which would essentially be the landing stage capability.

After engaging the atmosphere, the heating rates and deceleration loads would be excessive so that a successful propulsive abort would not be possible along the nominal trajectory, without substantial weight penalties, until the velocity has decayed to near the terminal conditions.\* Depending on the time after entry, however, a full aerodynamic liftup maneuver could be employed causing the vehicle to skip back to a higher altitude where the heating rates and decelerations are sufficiently low. It was estimated that 300,000 feet would be a minimum altitude since the vehicle velocity would still be high, although even if 150,000 feet were chosen, it would only represent another 10 seconds of time. The effect of this pull-up maneuver is illustrated in Figure (25) using the heavy vehicle undershoot trajectory in the VM-8 atmosphere. The maximum skip altitude reached after the pullup is presented versus the time the pull-up is initiated after entry. Until about 170 to 180 seconds after entry, this maneuver can be used. After this time, there is no safe abort mode to "backup" the primary entry sequence with the exception of eliminating the landing phase so that no surface contact would result.

For a period of time representing about 50 to 60% of the entry time there is probably no safe abort "backup" either aerodynamic or propulsive. The mission would proceed through

---

\*Designing the ascent stage to a severe heating environment could be extremely penalizing. In addition, the landing system would at most be capable of providing a 1.5 to 2 G acceleration while the ascent stage would be on the order of a fraction of 1 G. Providing a several G capability for abort would not be realistic.

the nominal sequence until the vehicle has decelerated sufficiently to fire the landing stage. Although the surface touchdown phase can be eliminated, the question of orbital rendezvous compatibility resulting from ascent at that time will require additional study.

## 7.2 Terminal Retro Landing

When the vehicle has slowed down sufficiently, the landing stage rockets will be fired to provide for a controlled soft touchdown on the surface. The conditions prior to landing stage firing based on the VM-8 atmosphere are presented in Figures (26) and (27). As pointed out previously, the VM-7 atmosphere actually results in the highest terminal velocities so that the velocities in Figure (26) could be about 30% higher at the 10,000 foot altitude level. Nevertheless, the conditions in Figures (26) and (27) do illustrate some significant points.

1. The flight path angle at retro fire will be quite shallow: on the order of  $-8$  to  $-10^\circ$  for the heavy vehicle and  $-15$  to  $-20^\circ$  for the light vehicle.
2. The constant altitude maneuver acts as a filter which essentially uncouples the landing mode from the initial entry conditions. The only significant differences show up due to the vehicle characteristics.
3. The low-speed equilibrium glide solution, i.e.,  $(\text{LIFT})^2 + (\text{DRAG})^2 = (\text{WEIGHT})^2$ , does not provide an accurate estimate of the velocity at low altitudes for the heavy vehicle since it is still in a transient state and never achieves equilibrium.

Additional study is required to determine the effects of lift and drag attenuation due to rocket engine firing on the landing maneuver.<sup>1</sup> The advantages and disadvantages of employing parachutes or other decelerators to augment the vehicle aerodynamic deceleration could be dependent on the extent of this attenuation.

## 7.3 Propulsive Range Make-up

Although it is most desirable to use aerodynamic control to the greatest extent possible, guidance errors will require some propulsive range make-up to successfully execute a surface rendezvous. The propulsive  $\Delta V$  expenditure per statute mile during horizontal translation, shown in Figure (28), varies inversely with surface velocity. Twice the translational velocity must be added to this  $\Delta V$  to account for the acceleration and deceleration periods.

If the translational velocity is held to 50 miles per hour, the total propulsive penalty is on the order of 1,000 fps per statute mile. This transforms to about a 10% weight penalty per statute mile for an  $I_{sp} = 325$  seconds. The total  $\Delta V$  can be reduced to about 720 fps (for the first mile traveled, although increasing as the square root of range) by optimizing the translational velocity. The optimum velocity, however, can be quite large: for the first mile, the velocity would be about 125 fps, but like  $\Delta V$ , also increases as the square root of range.

A ballistic, parabolic path would require less  $\Delta V$  than the horizontal path but would probably require more complicated guidance and control. For large ranges, however, the horizontal penalties would become quite large and a ballistic path would have to be considered.

For the low speed horizontal translation, the effect of the atmosphere (drag) is quite small, as indicated in Figure (28) for the VM-4 high density model.

## 8.0 CONCLUSIONS

1. Manned ballistic entry into Mars is possible from a highly elliptical orbit. However, the landing propulsion is very sensitive to ballistic parameter, accurate entry guidance is required and large surface landing site dispersions are inherent.
2. An Apollo shape or blunt cone lifting entry vehicle provide sufficient aerodynamic performance for direct entry of the MINIMEM vehicles at 25,000 fps with an entry corridor of 10 n.m. and a maximum deceleration of 10 G's. A direct entry undershoot limit of less than 9 G's is probably not possible unless the entry corridor can be made less than 10 n.m., or the negative lift overshoot criterion is used. The negative lift overshoot criterion requires accurate knowledge of position within the corridor.
3. The direct entry mode requires more accurate guidance and more flexibility in entry trajectory control to achieve a desired landing site than out-of-orbit entry. In the case of out-of-orbit entry, all range errors resulting from the initial entry corridor could probably be corrected after the vehicle exits the blackout period. In addition, the deceleration limits can be maintained as low as 3 to 4 G's from out-of-orbit entry in order to minimize the support structure of the manned capsule compartment.

4. The heat protection system and structural weights for direct entry would represent less than 15% of the gross weight for the heavy (2 man) MINIMEM, and about 30% for the light (1 man) MINIMEM. These weight requirements would be somewhat less for out-of-orbit entry due to the lower G's, lower heating and the possibility of employing low density ablator material.
5. From a comparison between the light MINIMEM and unmanned (ballistic) MSSR, the entry time for the MINIMEM entry at 25,000 fps can be as much as 4 times the MSSR entry at 32,000 fps. This implies about twice as much insulation (and non-pyrolyzing ablator material) for the MINIMEM. On the other hand, the 10 G limit on the MINIMEM compared to the 40 G limit on the MSSR would result in larger structural weight for the MSSR.
6. Aborting the direct entry mission by utilizing the landing stage propulsion system is possible at any time up to about 100 seconds before nominal entry in the VM-8 atmosphere without significant heating. Although post abort rendezvous was not analyzed, all the ascent propellant would be available to make substantial  $\Delta V$  changes. An abort after atmospheric entry would require full positive lift in order to skip to a high enough altitude to use propulsion. However, for about 50% of the entry time, there is not sufficient aerodynamic control left to perform the skip maneuver.
7. The terminal landing propulsion requirements are essentially independent of the entry velocity and entry mode, and only depend on the vehicle characteristics and atmospheric properties. In addition, propulsive range make-up results in weight penalties on the order of 10% of the vehicle weight per mile employing horizontal translation. For large range errors a ballistic trajectory would be required.

#### 9.0 RECOMMENDATIONS FOR FURTHER STUDY

1. Entry guidance accuracies (including corridor width and position certainties) from direct approach and out-of-orbit entries require detailed analysis.
2. Relative surface area accessibility from direct approach and out-of-orbit entry require detailed comparison.

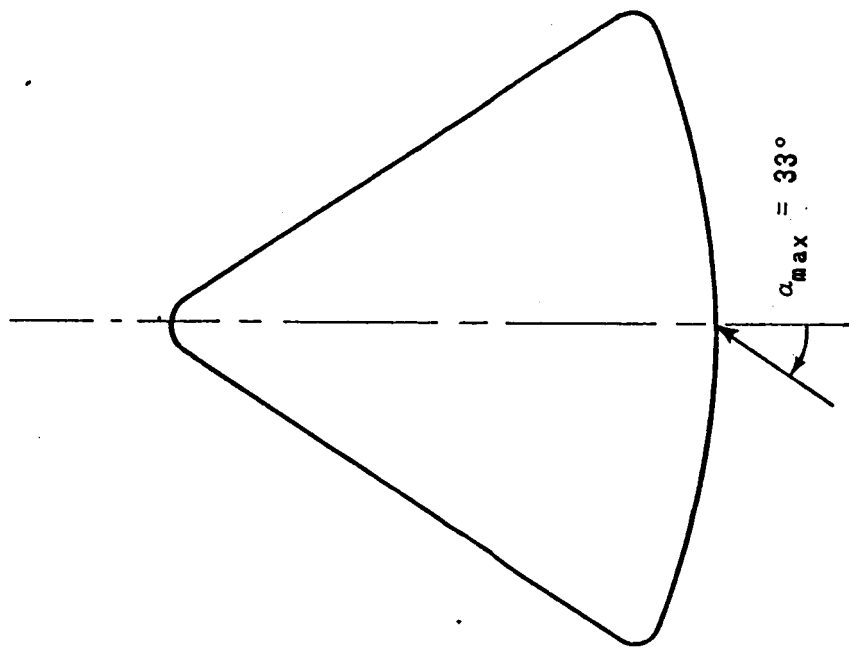
3. The unmanned MSSR should be investigated as a lifting vehicle at the twilight flyby entry velocities. This would then provide a better basis for MSSR/MINIMEM commonality.

1013-DEC-sjh

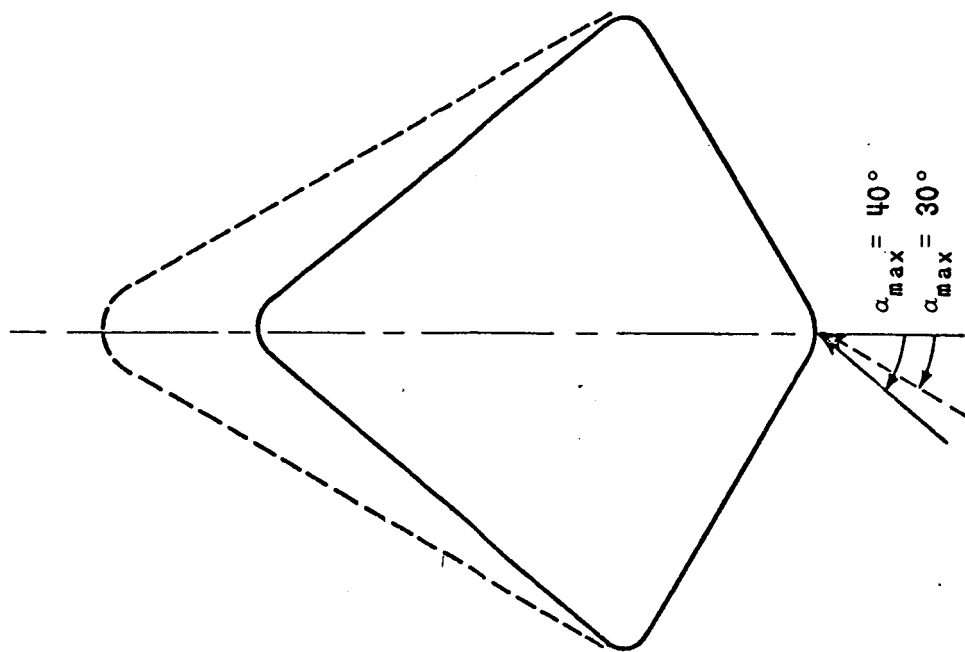
*Handwritten signature: D. E. Cassidy*  
D. E. Cassidy

REFERENCES

1. Unmanned MSSR Entry into Mars during the 1975 Manned Twilight Flyby, Bellcomm TM-67-1013-7, D. E. Cassidy, dated September 20, 1967.
2. Conceptual Design of Structural and Propulsion Systems for an MSSR Rendezvous Vehicle - Case 103-2, by D. Macchia, M. H. Skeer and J. Wong, dated August 5, 1966.
3. MSSR/MEM Commonality - Case 233, Bellcomm Memorandum for File, by D. E. Cassidy and H. S. London, dated July 19, 1967.
4. Preliminary Sizing of a Mars Excursion Module Ascent Capsule Based on Mercury Spacecraft Design - Case 233, Bellcomm Memorandum for File, by M. H. Skeer, dated September 25, 1967.
5. Apollo Reentry Heating as a Function of Angle-of-Attack, MSC Internal Note No. 64-ET-55, NASA, Manned Spacecraft Center, August 14, 1964.
6. Definition of Experimental Tests for a Manned Mars Excursion Vehicle, North American Rockwell Corp., Space Division, SD 67-755-1, Contract NAS9-6464, January 12, 1968.
7. Superlight Ablative Systems for Mars Lander Thermal Protection, Eric L. Strauss, AIAA/ASME 8th Structures, Structural Dynamics and Materials Conference, Palm Springs, Calif., March 29-31, 1967.



(APOLLO TYPE)



(60° CONE)

FIGURE 1 - CAPSULE CONFIGURATIONS

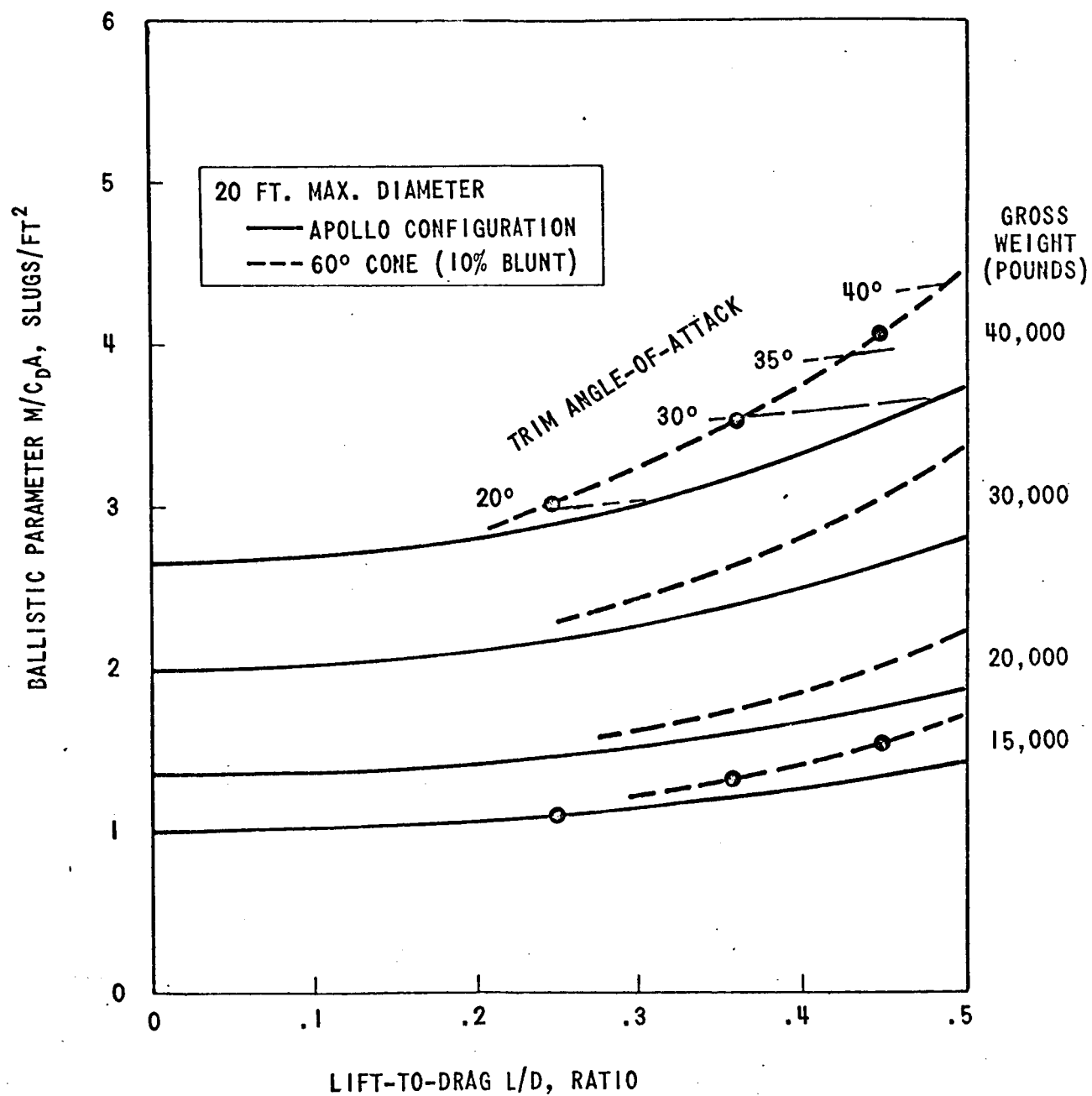


FIGURE 2. - BALLISTIC PARAMETER vs. LIFT-TO-DRAG RATIO



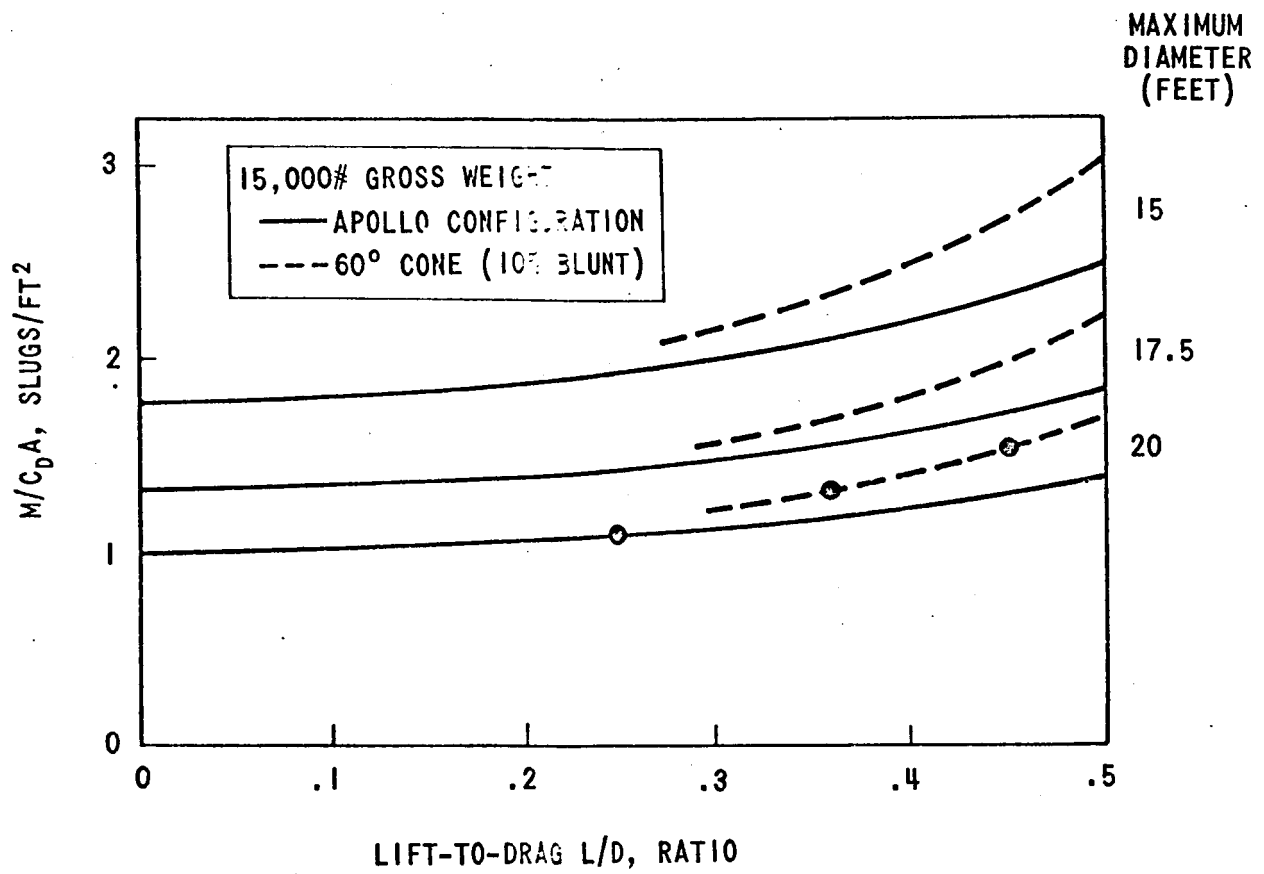


FIGURE 3 - BALLISTIC PARAMETER vs. LIFT-TO-DRAG RATIO

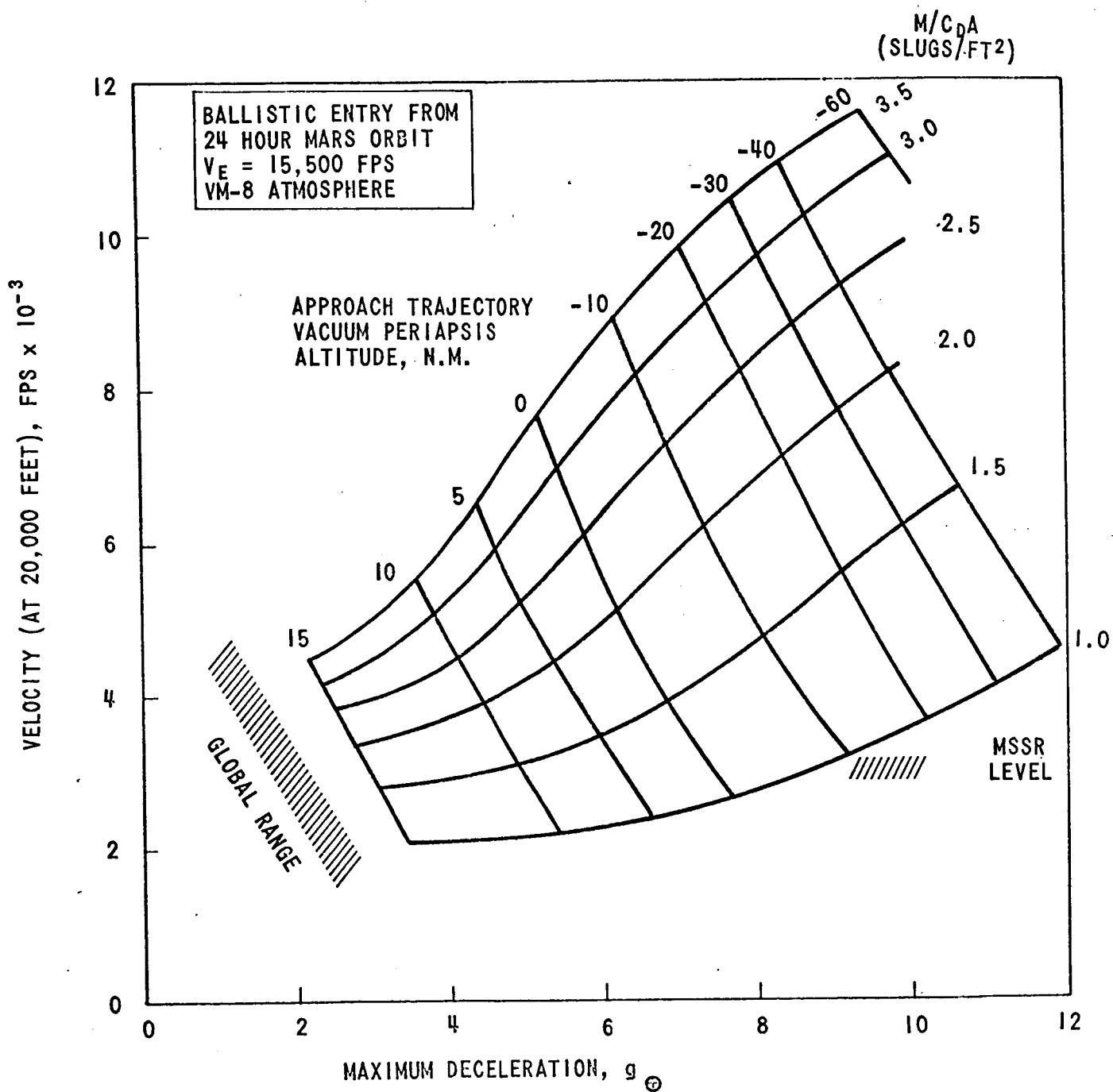


FIGURE 4 - VELOCITY AT ALTITUDE vs. MAXIMUM DECELERATION

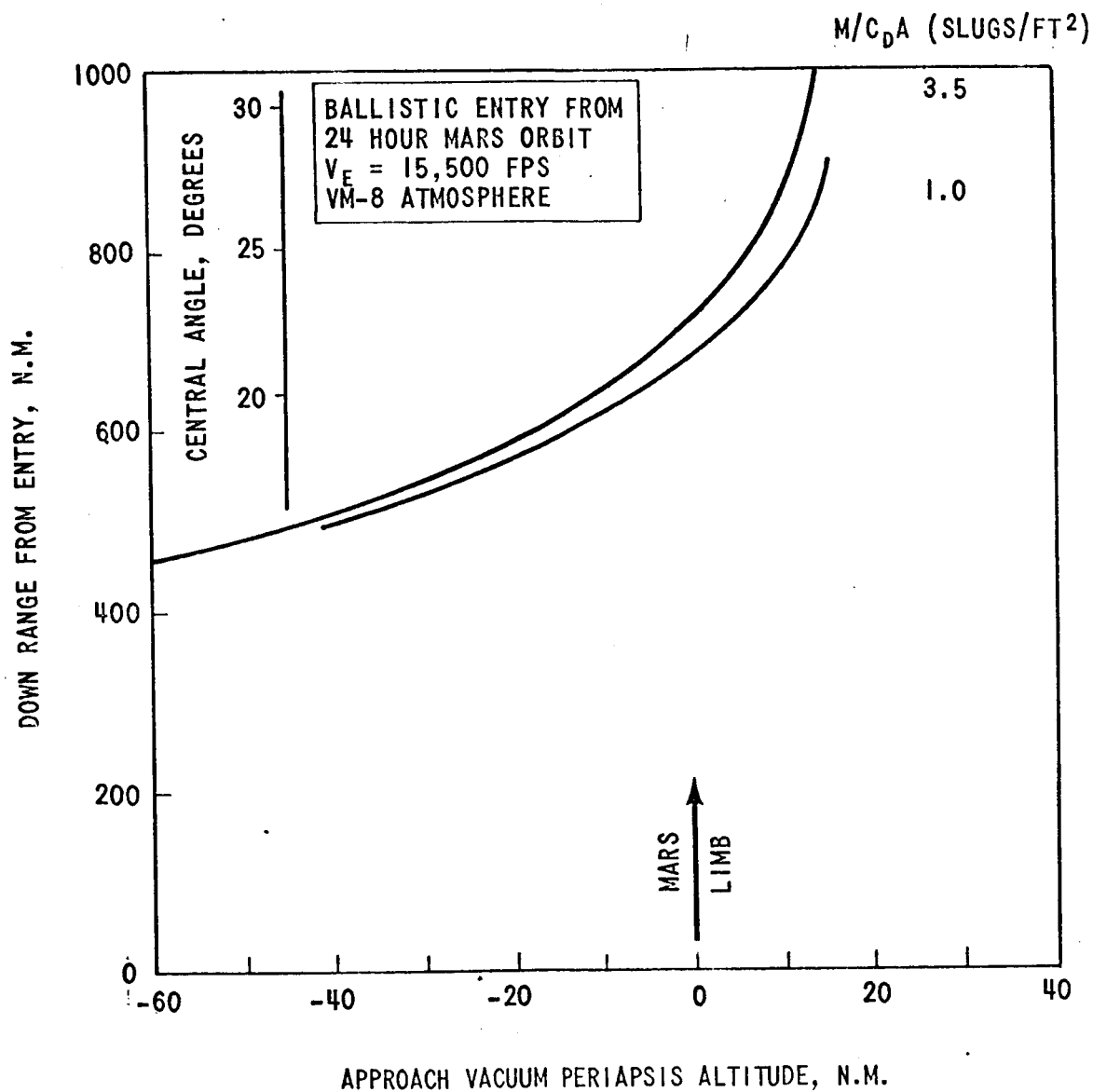


FIGURE 5 - DOWN RANGE FROM ENTRY

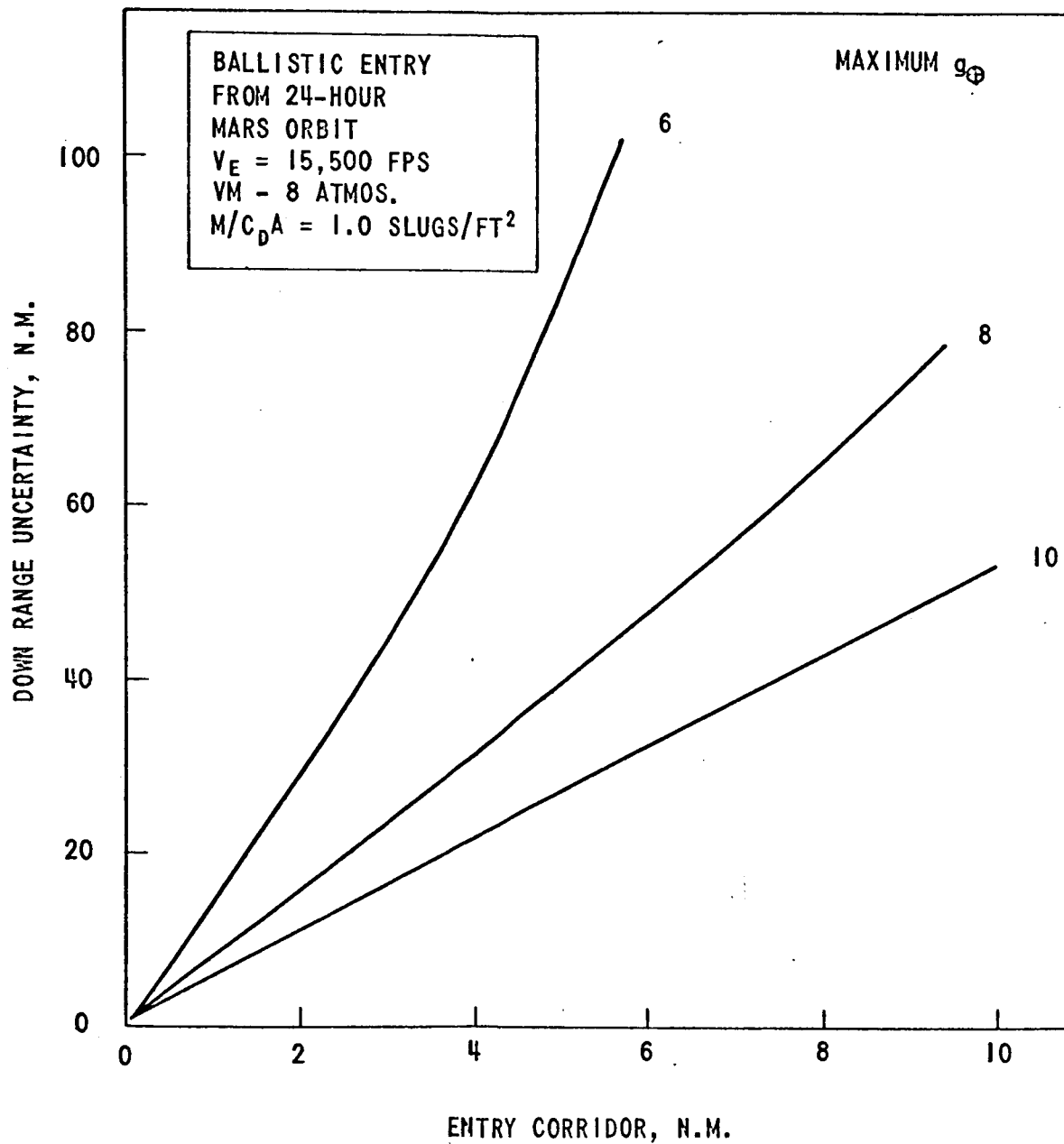


FIGURE 6 - RANGE UNCERTAINTY vs. ENTRY CORRIDOR

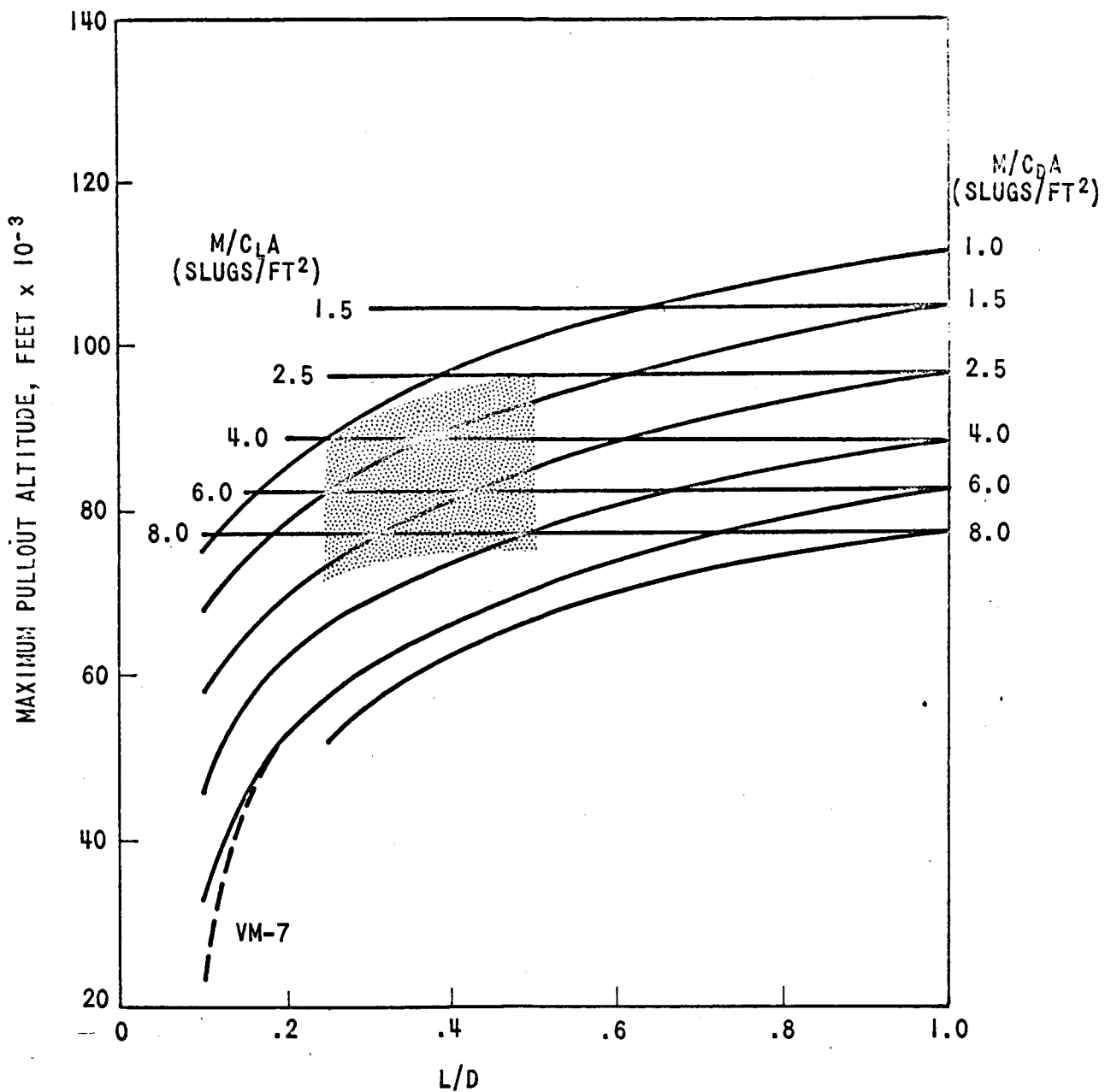


FIGURE 7 - MAXIMUM PULLOUT ALTITUDE IN THE VM-8 ATMOSPHERE

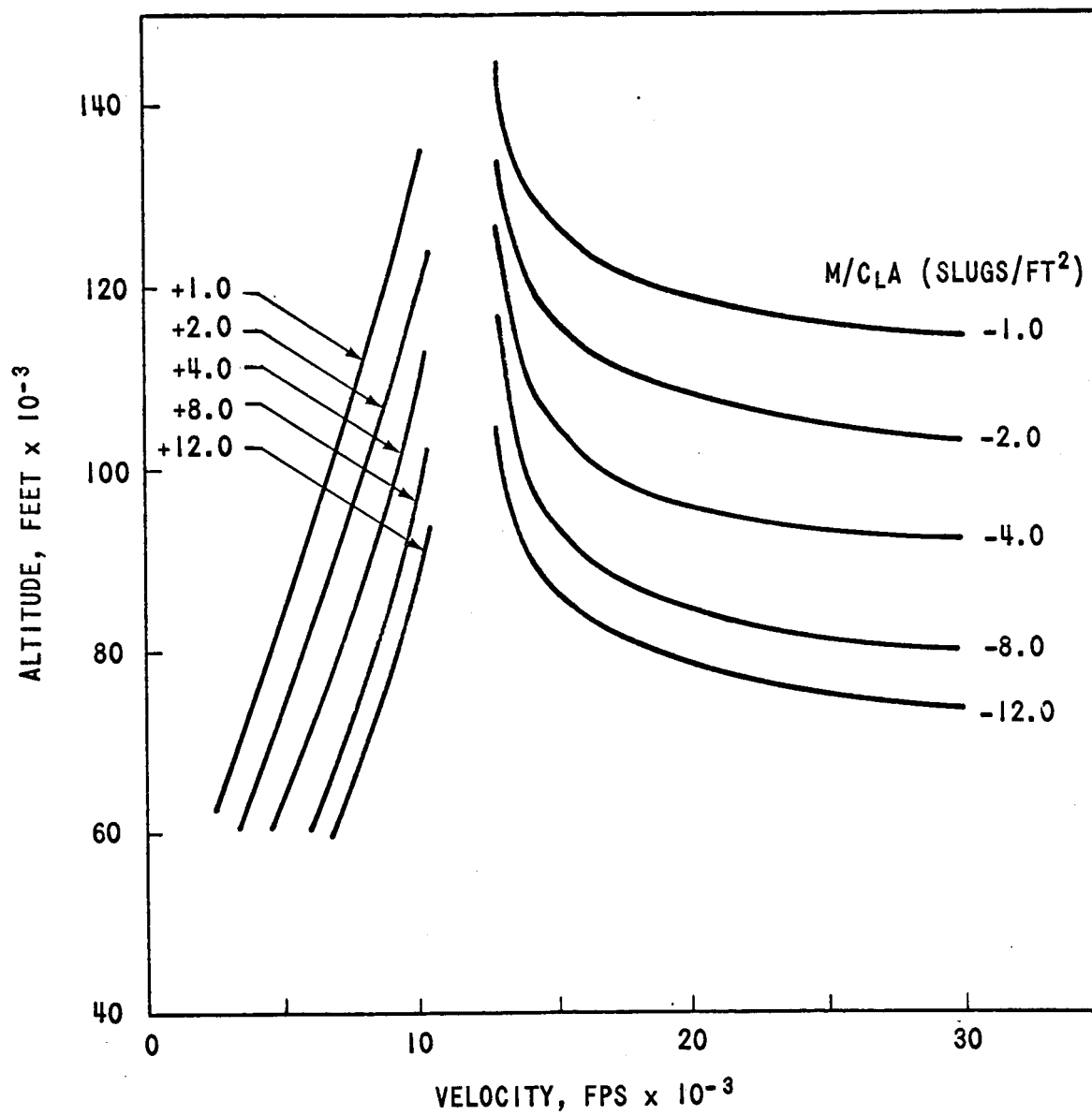


FIGURE 8 - EQUILIBRIUM GLIDE IN THE VM-8 ATMOSPHERE

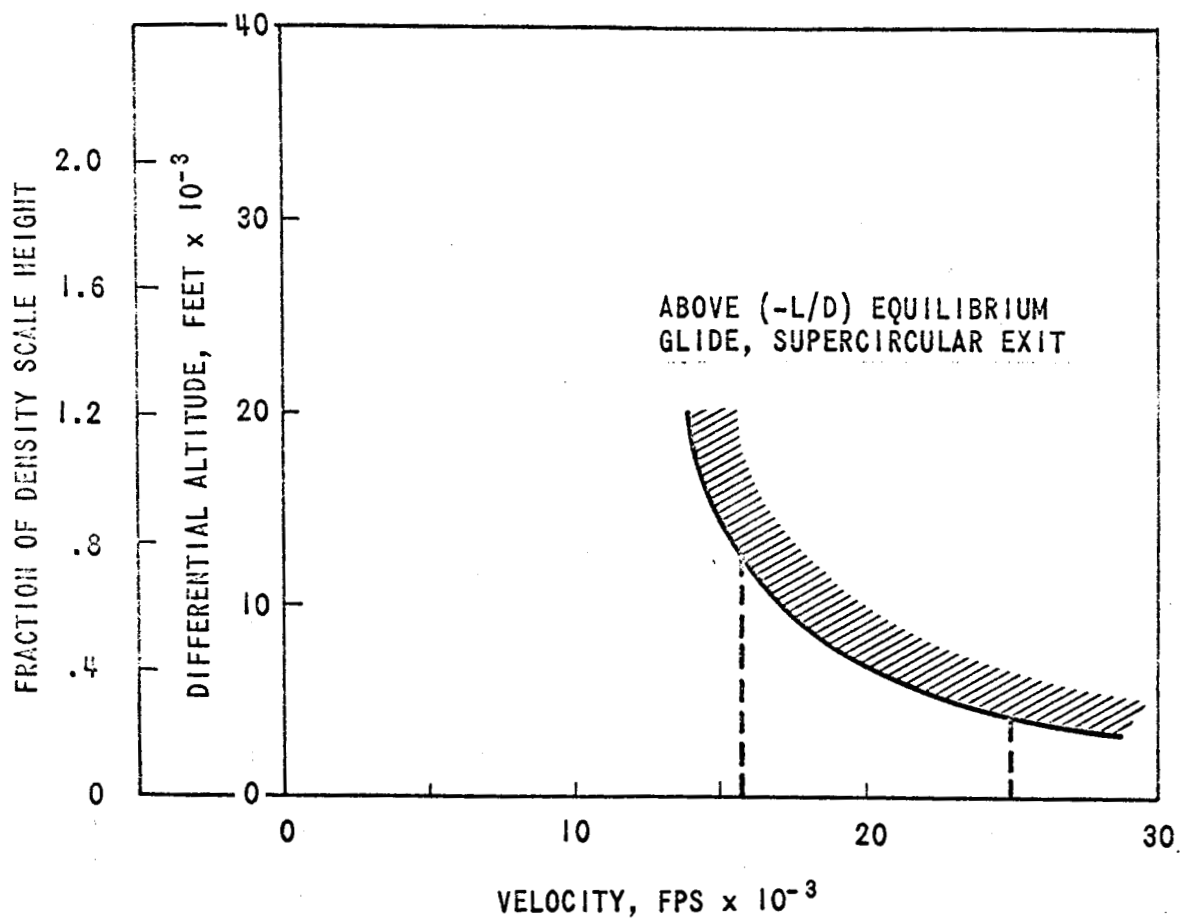


FIGURE 9 - DIFFERENCE IN EQUILIBRIUM GLIDE ALTITUDE AND MAXIMUM ALTITUDE (FIGURE 7), VM-8 ATMOSPHERE

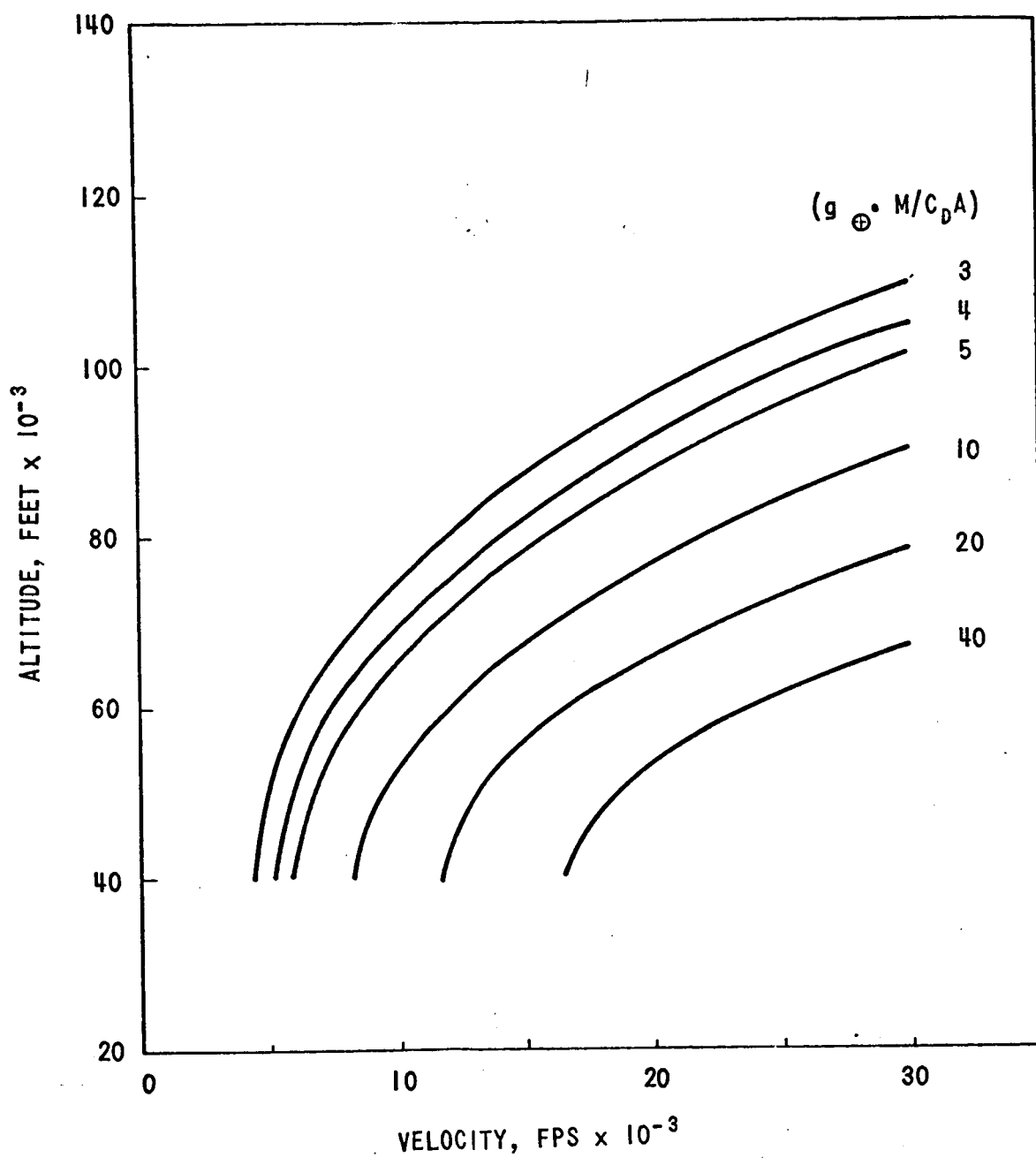


FIGURE 10 - LIMIT LOAD LINES IN THE VM-8 ATMOSPHERE



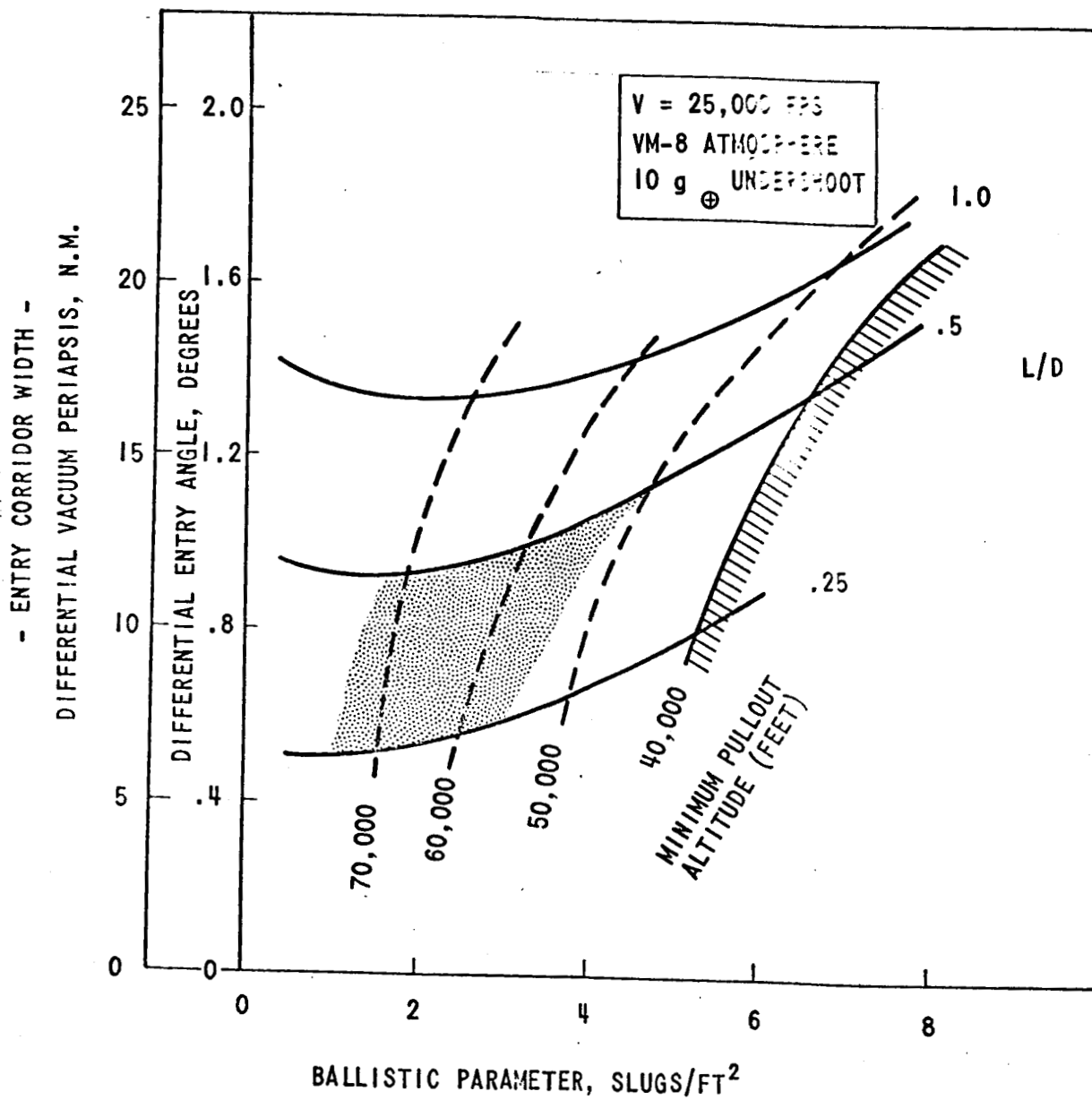


FIGURE 11 - ENTRY CORRIDOR vs. BALLISTIC PARAMETER, DIRECT ENTRY

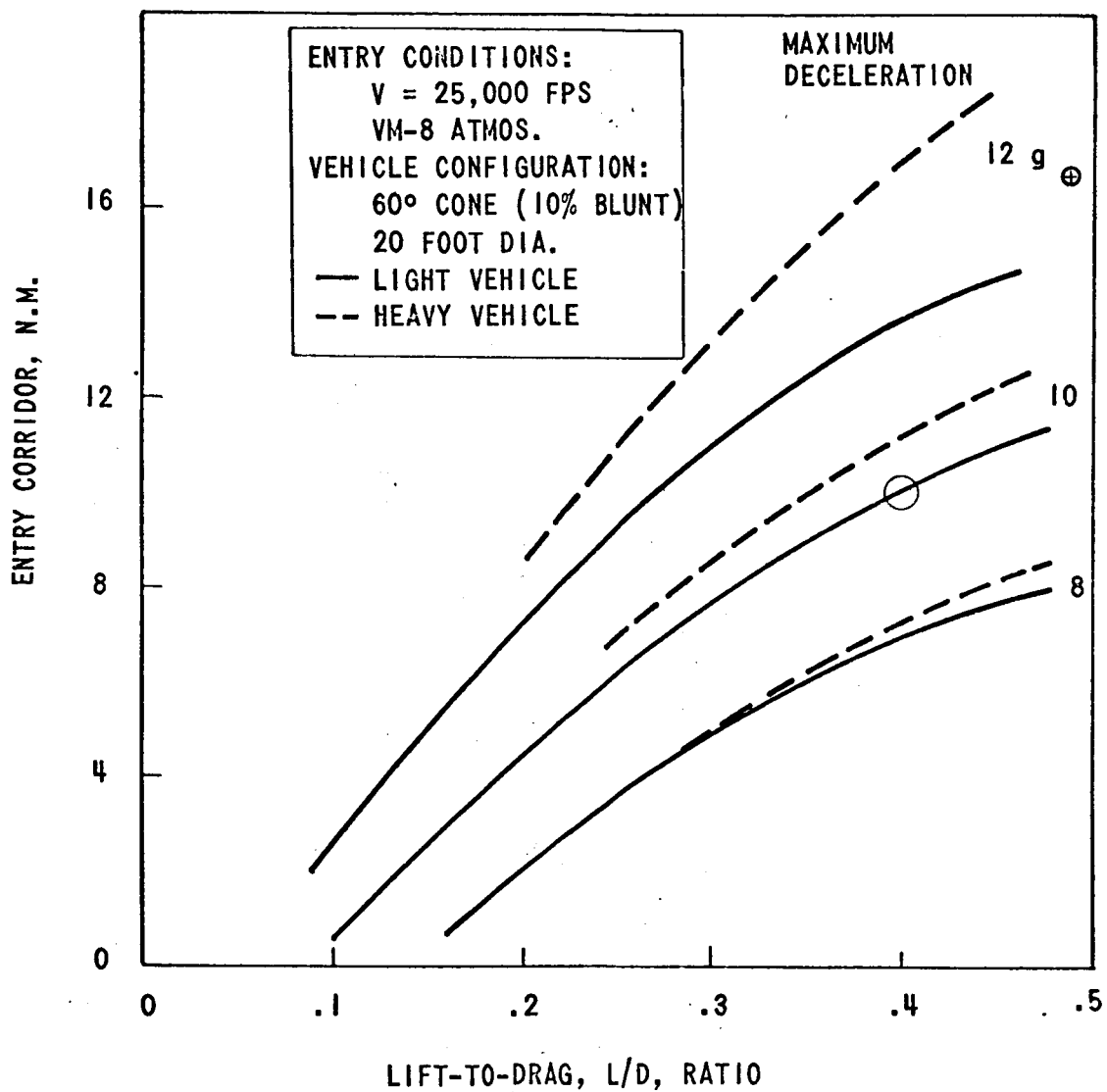


FIGURE 12 - ENTRY CORRIDOR vs. LIFT-TO-DRAG RATIO, DIRECT ENTRY

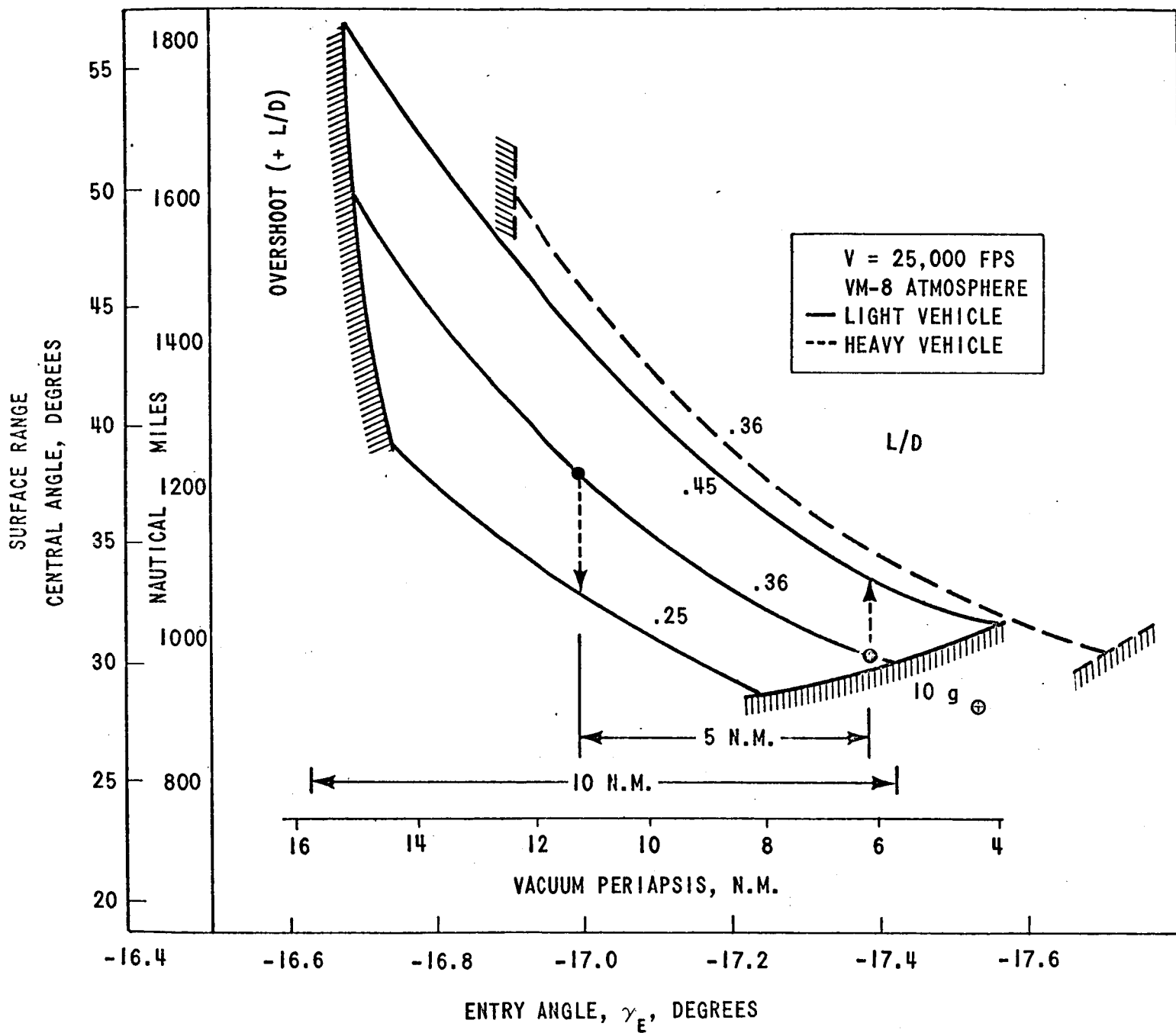


FIGURE 13 - SURFACE RANGE vs. ENTRY ANGLE FOR ROLL MODULATED, CONSTANT ALTITUDE MANEUVER, DIRECT ENTRY

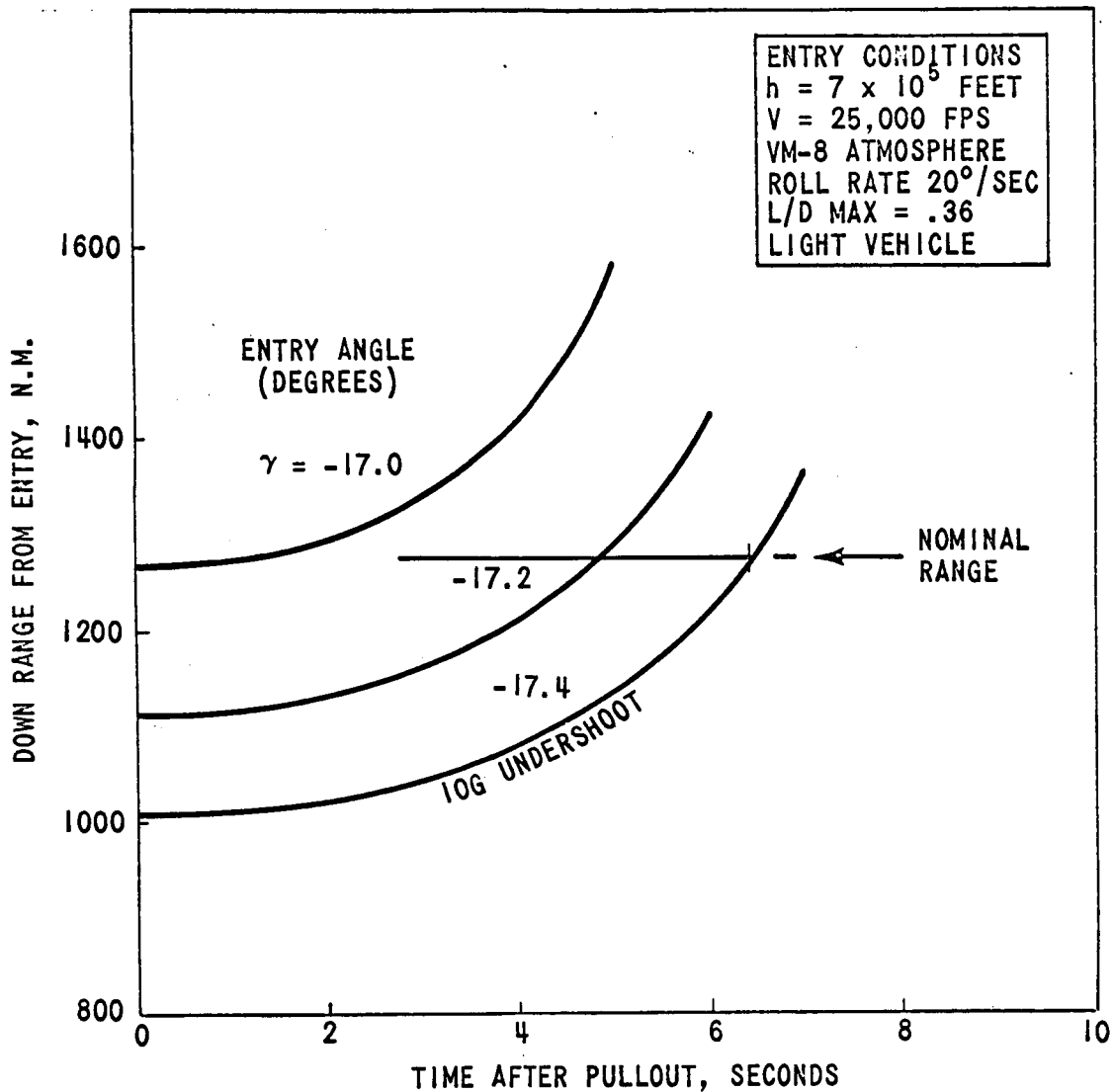


FIGURE 14 INCREASING SURFACE RANGE  
USING ROLL DELAY, DIRECT  
ENTRY

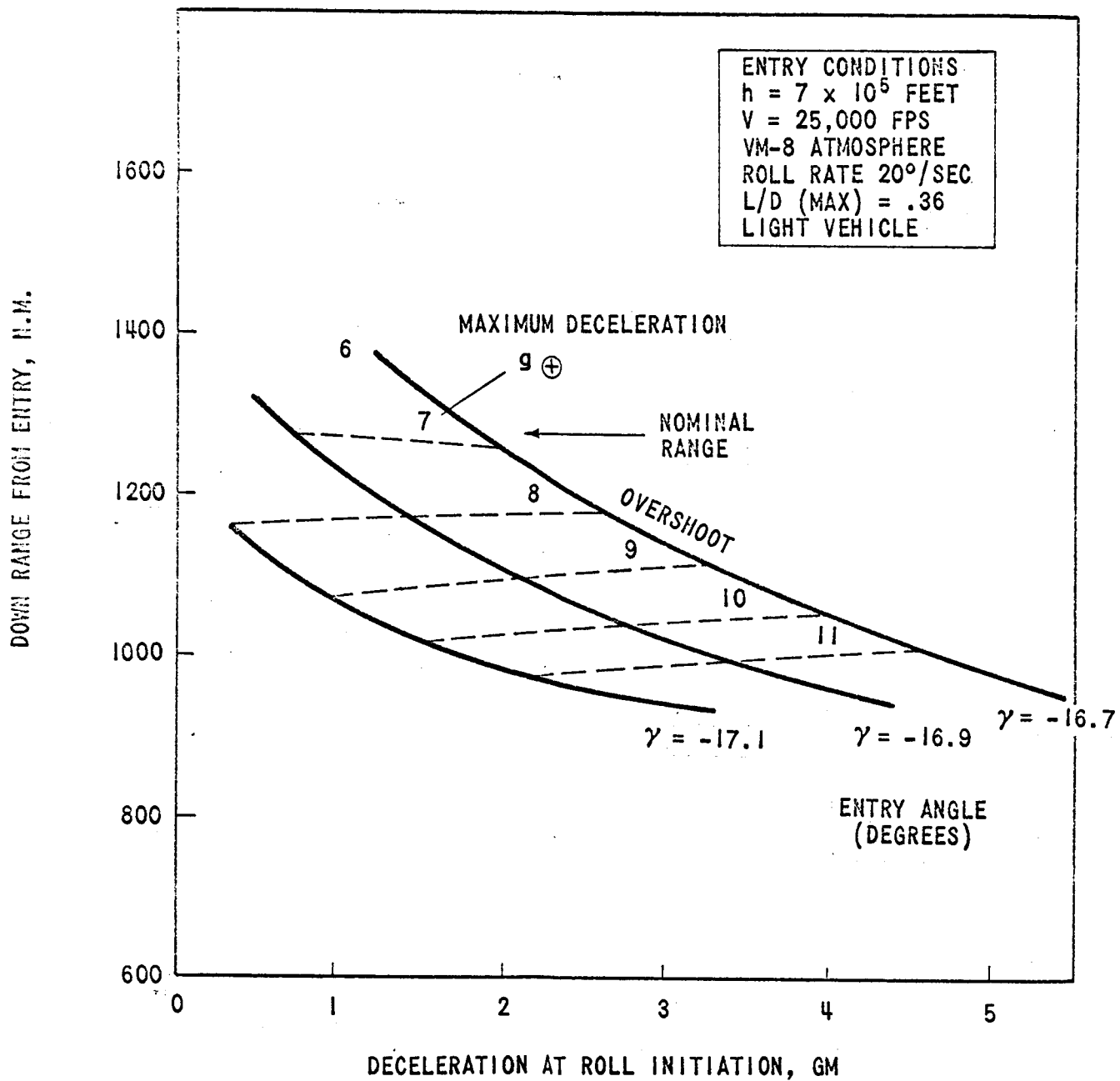


FIGURE 15 REDUCING SURFACE RANGE  
 USING NEGATIVE  $L/D$

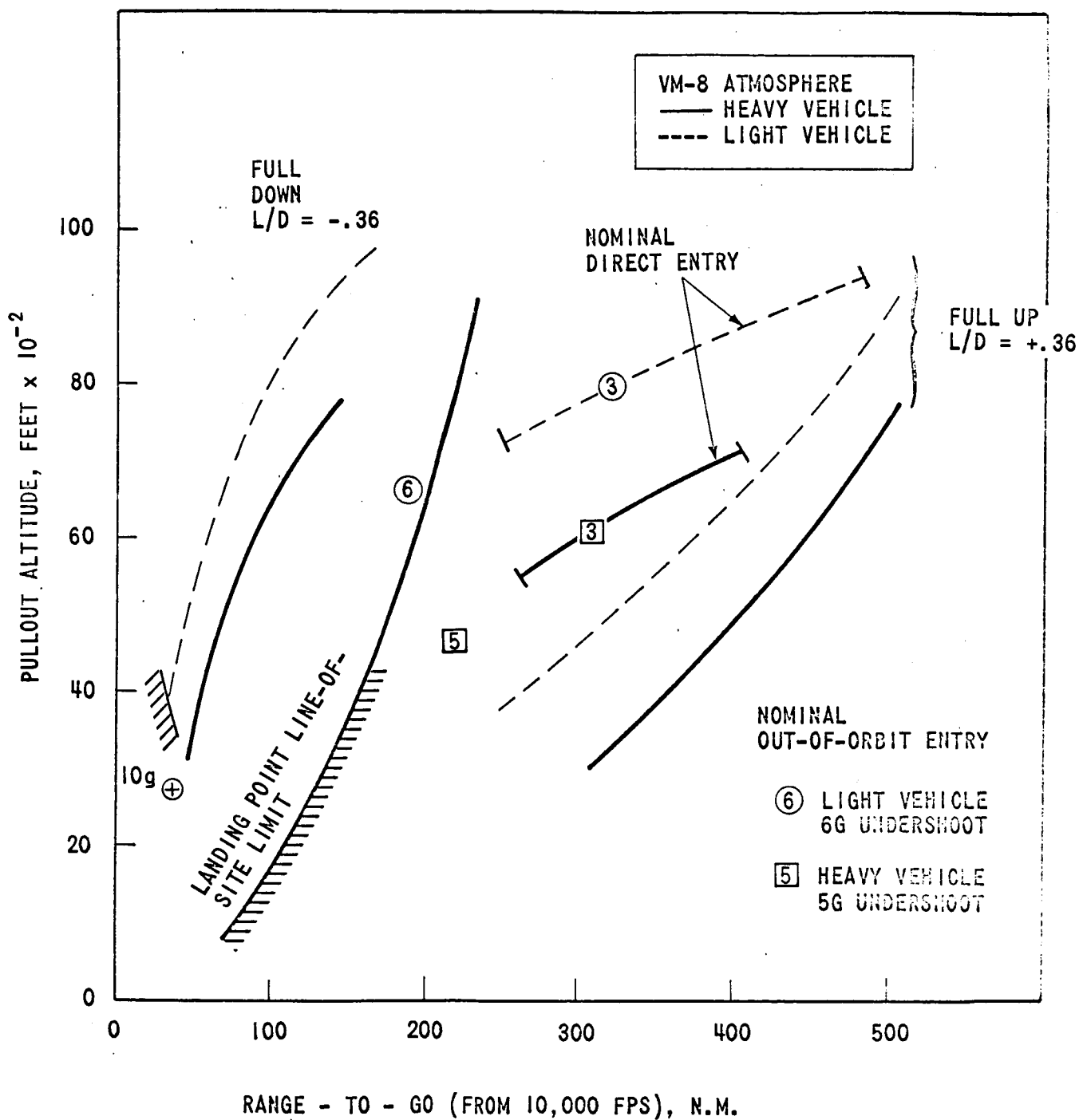


FIGURE 16 MAXIMUM SURFACE RANGE  
 CONTROL FROM THE POINT  
 WHERE VELOCITY = 10,000 FPS

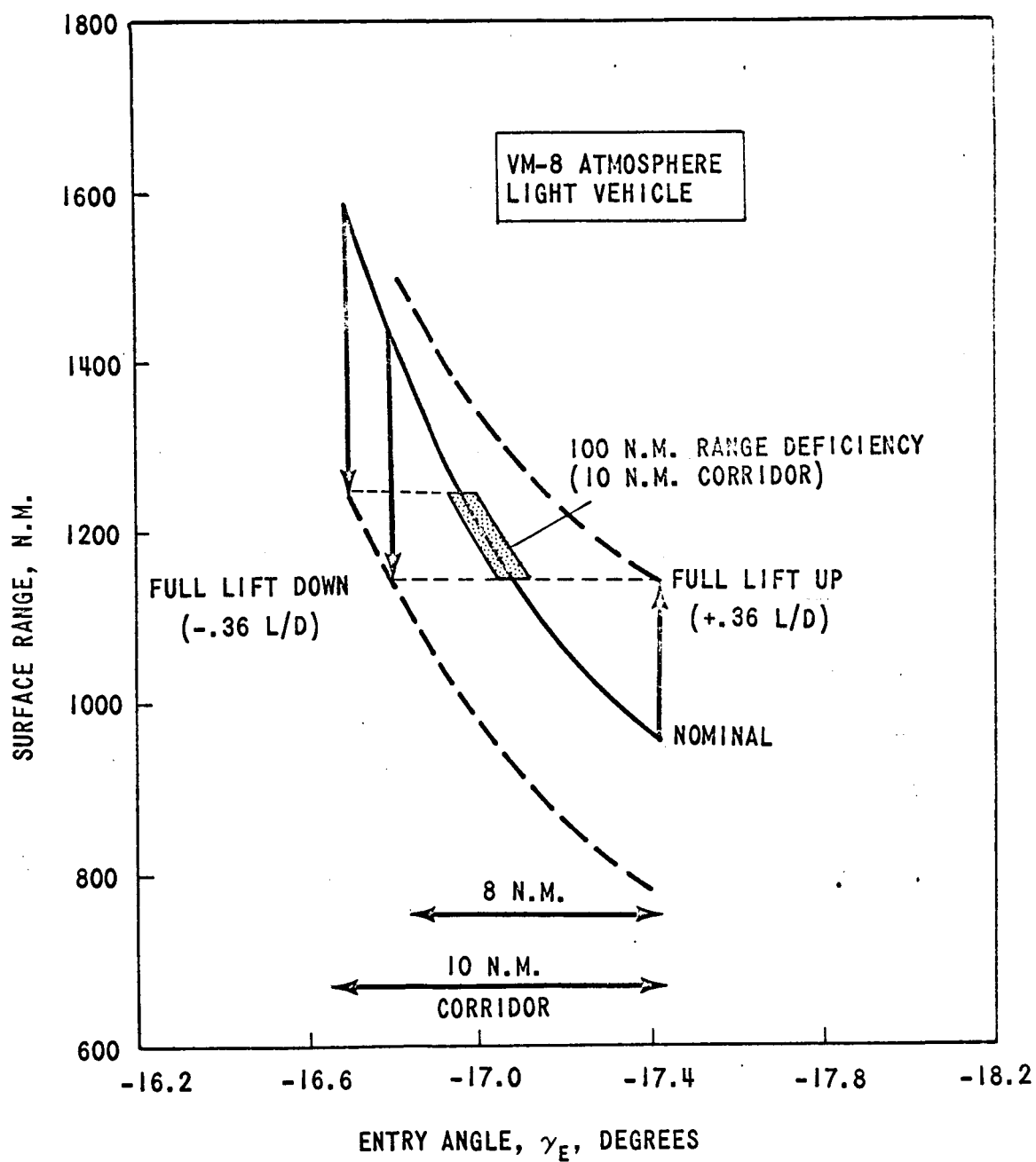


FIGURE 17 - SURFACE RANGE vs. ENTRY ANGLE FOR TRAJECTORY CONTROL AFTER VELOCITY REDUCES BELOW 10,000 FPS

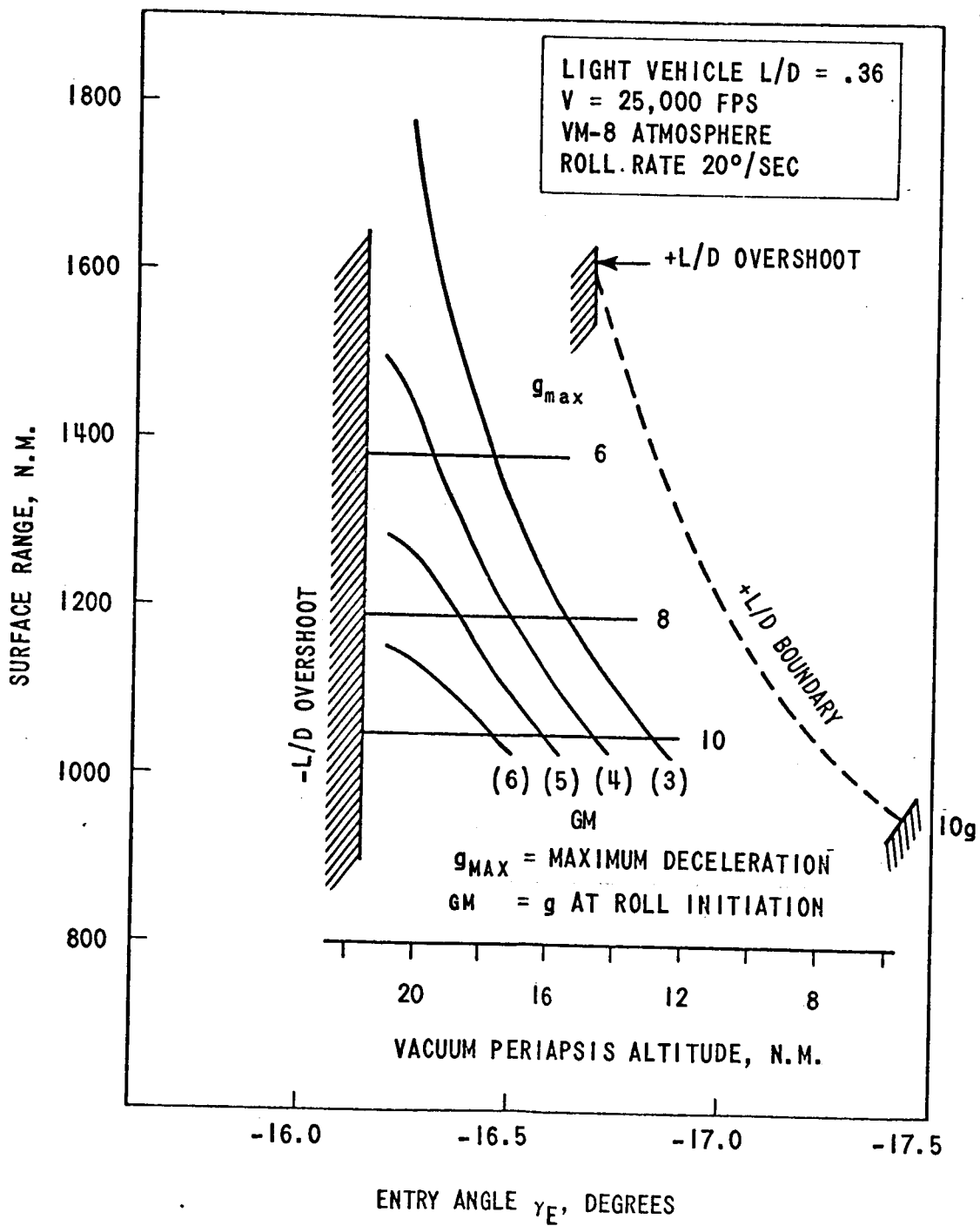
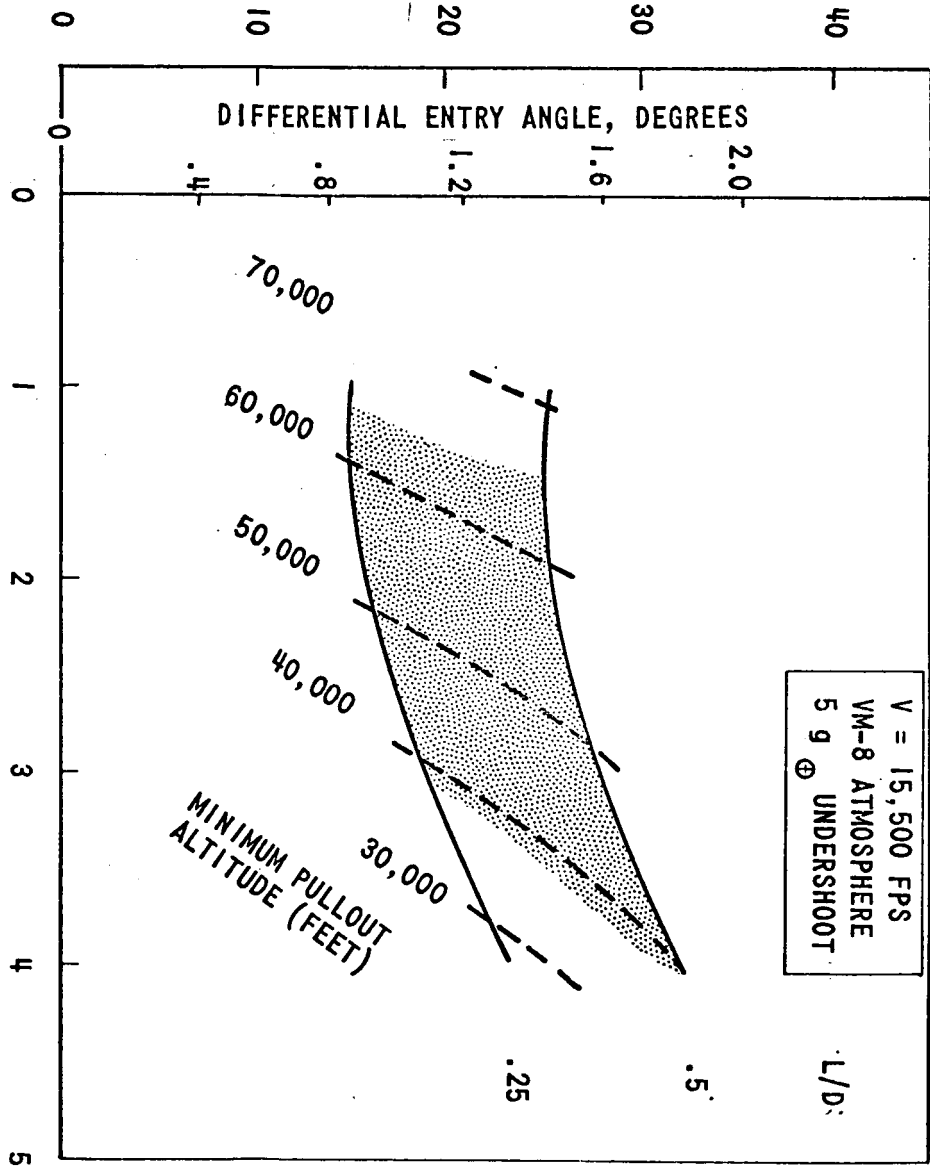


FIGURE 18 - SURFACE RANGE vs. ENTRY ANGLE, NEGATIVE LIFT OVERSHOOT



- ENTRY CORRIDOR -  
DIFFERENTIAL VACUUM PERIAPSIS, N.M.



BALLISTIC PARAMETER, SLUGS/FT<sup>2</sup>

FIGURE 19 - OUT-OF-ORBIT ENTRY CORRIDOR vs. BALLISTIC PARAMETER

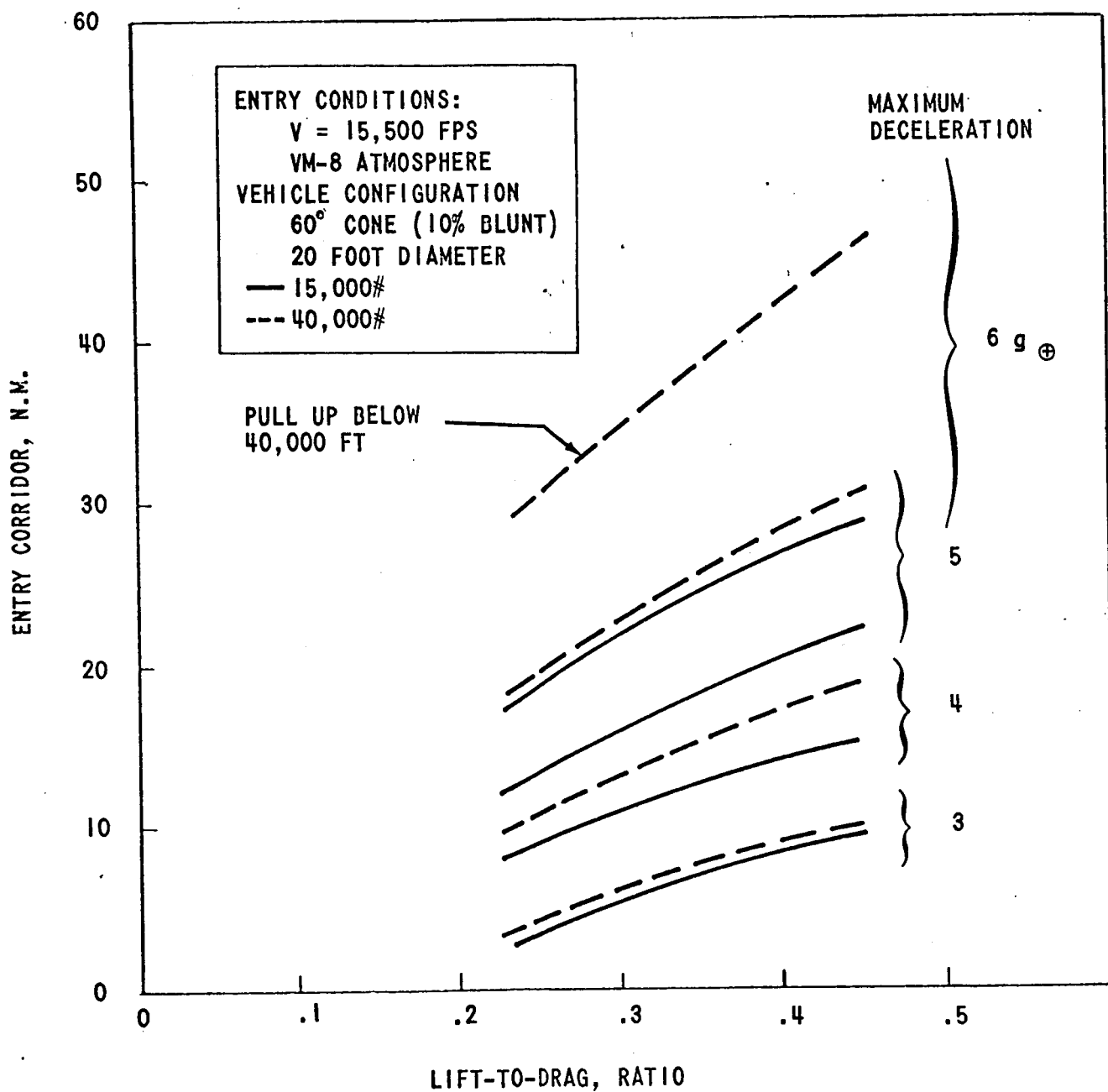


FIGURE 20 - OUT-OF-ORBIT ENTRY CORRIDOR vs. LIFT-TO-DRAG, RATIO

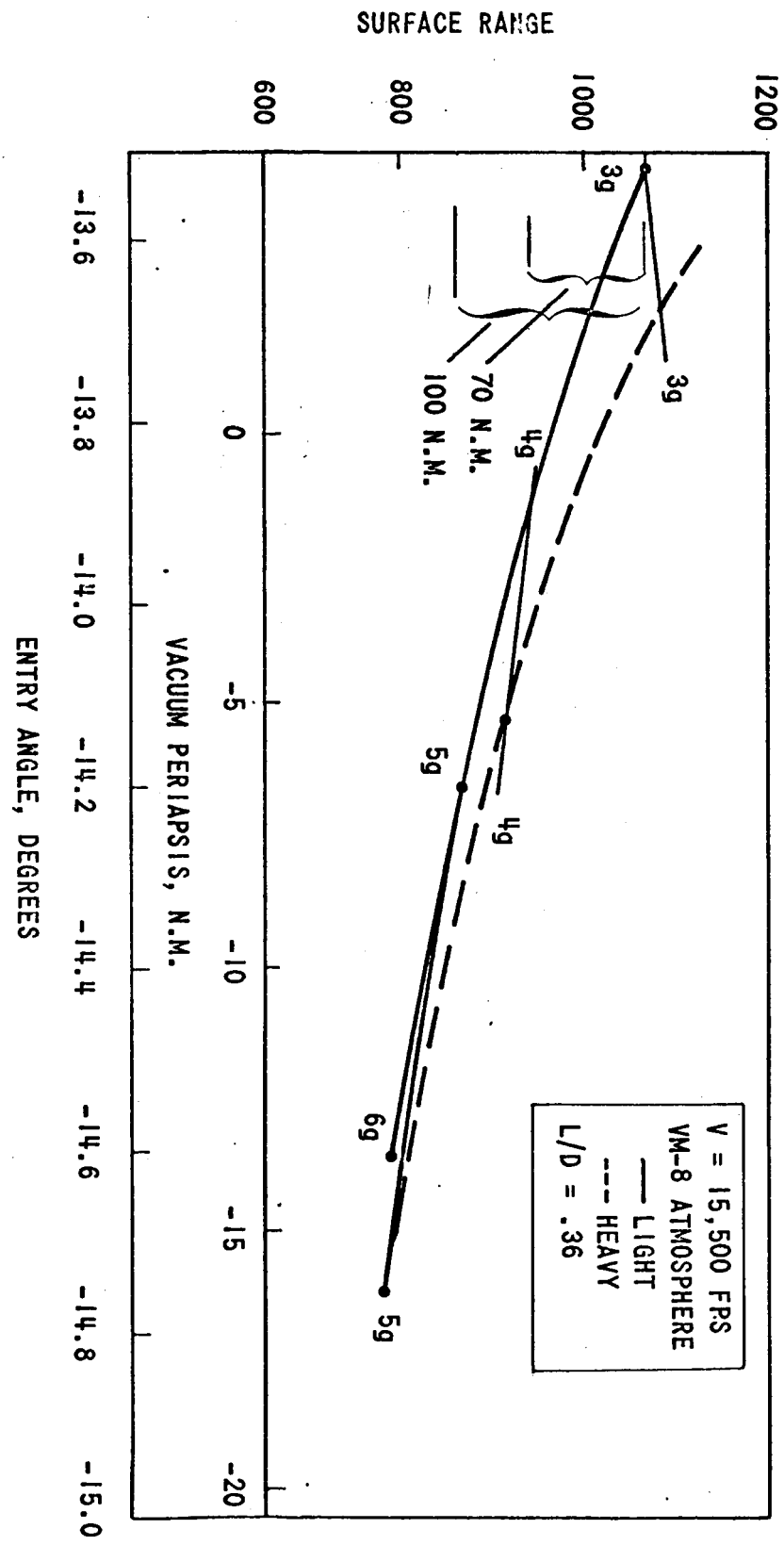


FIGURE 21 - SURFACE RANGE vs. ENTRY ANGLE, FOR ROLL MODULATED, CONSTANT ALTITUDE MANEUVER, OUT-OF-ORBIT ENTRY

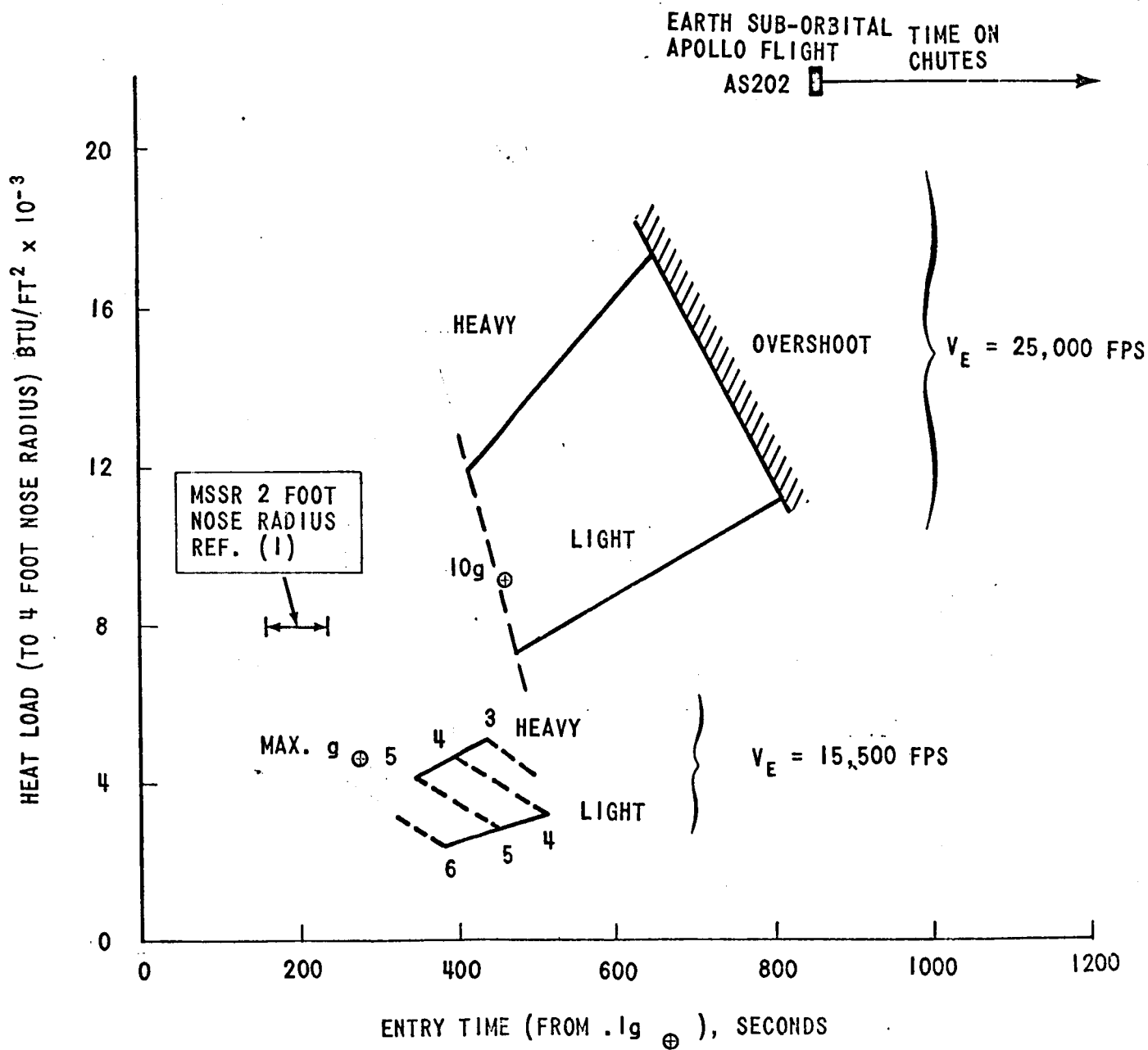


FIGURE 22 - STAGNATION POINT HEAT LOAD (4 FOOT EFFECTIVE RADIUS) vs. TIME FROM .1g ⊕, VM-8 ATMOSPHERE, L/D = .36

NOTES:

- 1 ABORT WITHOUT ENGAGING THE ATMOSPHERE UTILIZING LANDING AND/OR ASCENT STAGE PROPULSION.
- 2 ABORT UTILIZING AERODYNAMIC LIFT TO SKIP OUT OF THE ATMOSPHERE.
- 3 ABORT NOT POSSIBLE WITHOUT EXPERIENCING LARGE HEATING RATE AND LARGE DECELERATION LOADS.
- 4 ABORT IS ACCOMPLISHED BY ESSENTIALLY FOLLOWING THE LANDING SEQUENCE WITH THE POSSIBILITY OF ELIMINATING THE TOUCHDOWN.

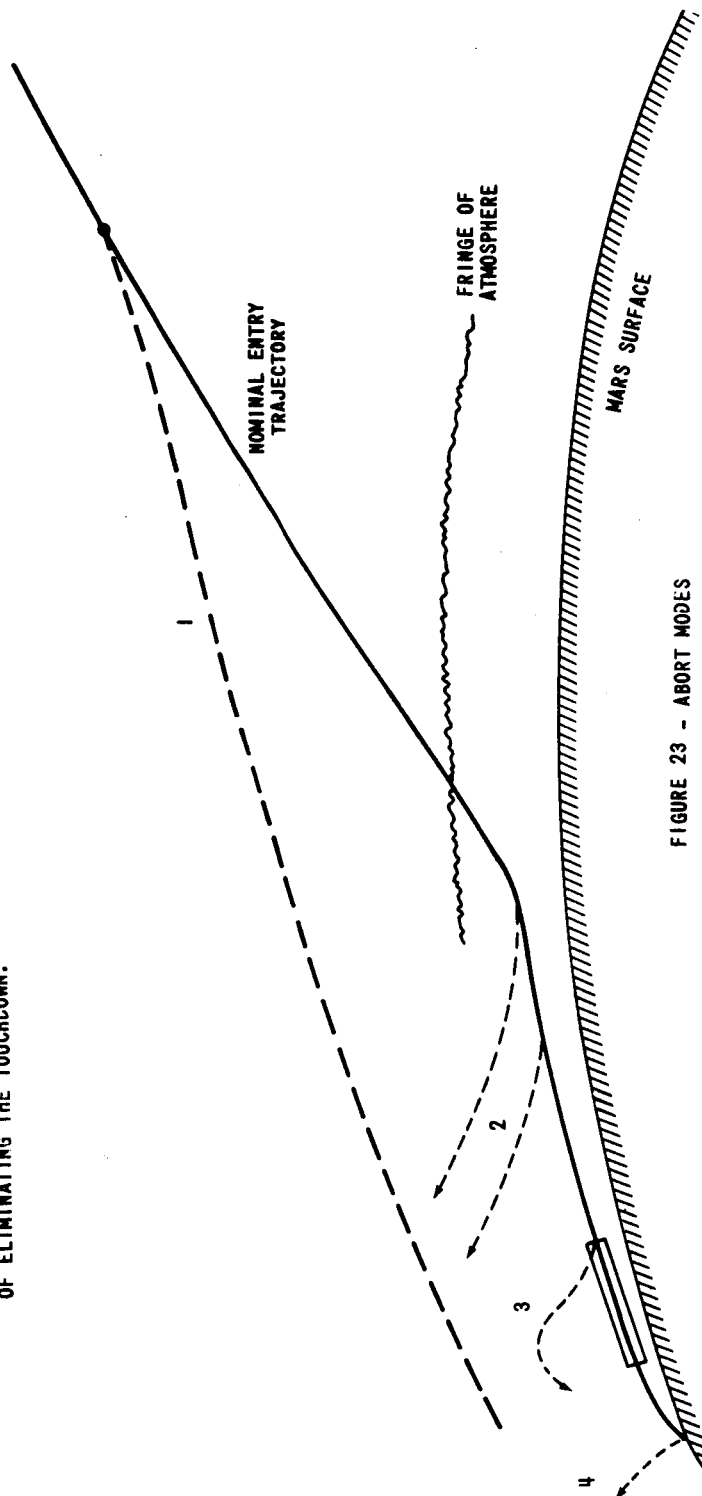


FIGURE 23 - ABORT MODES

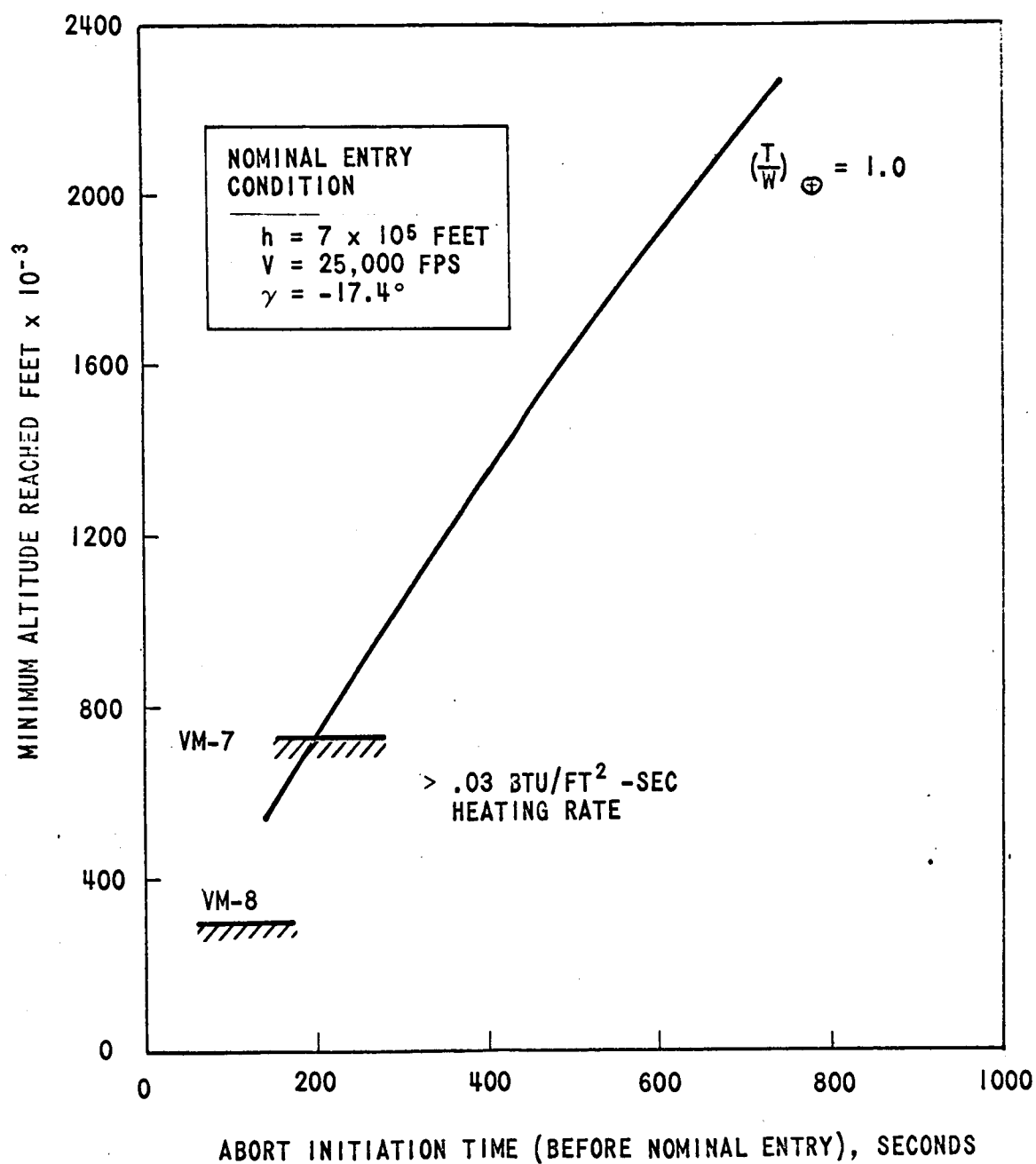


FIGURE 24 - PRE-ENTRY ABORT FOR DIRECT ENTRY

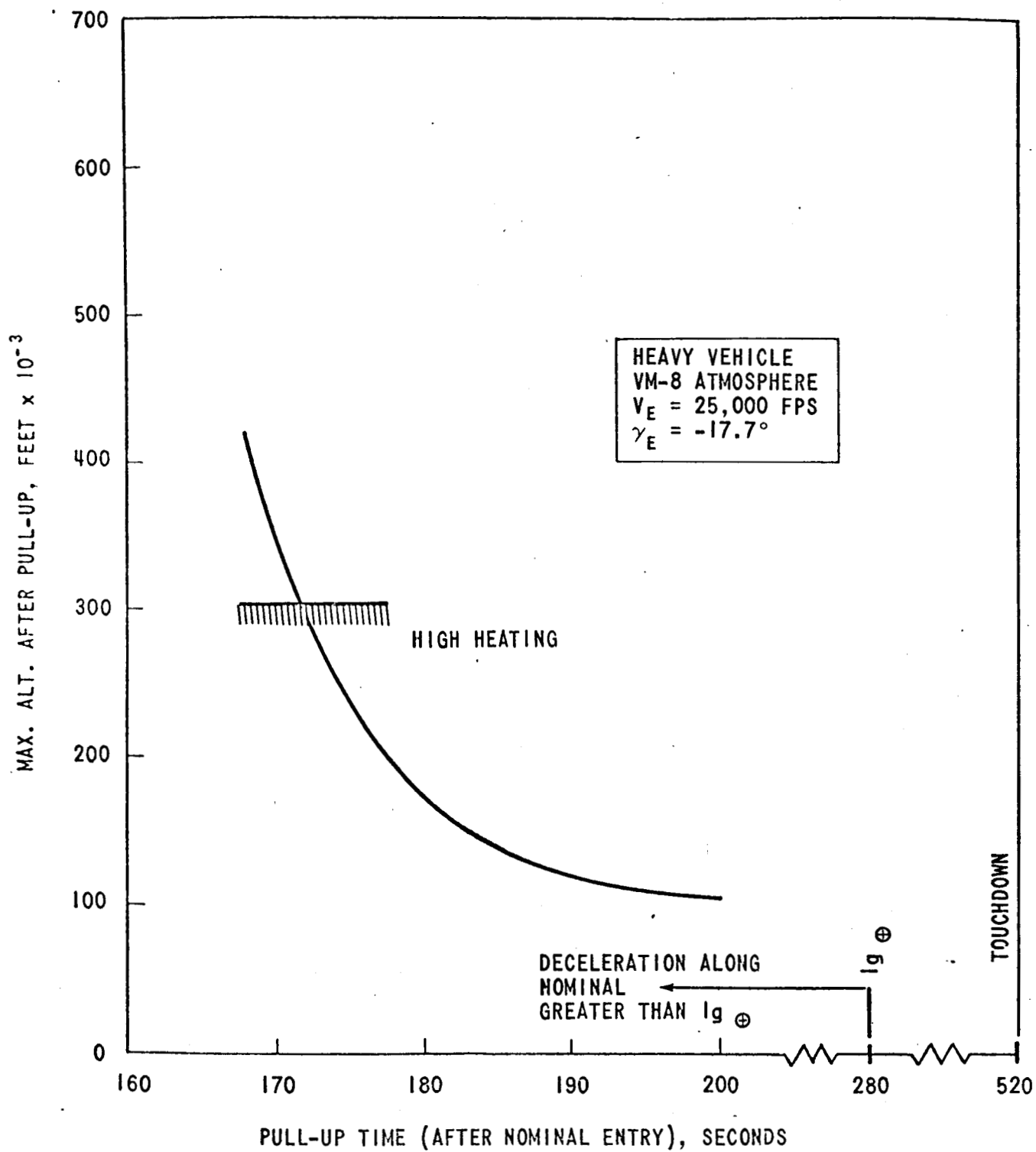


FIGURE 25 - MAXIMUM ALTITUDE REACHED AFTER PULL-UP (FULL POSITIVE LIFT)

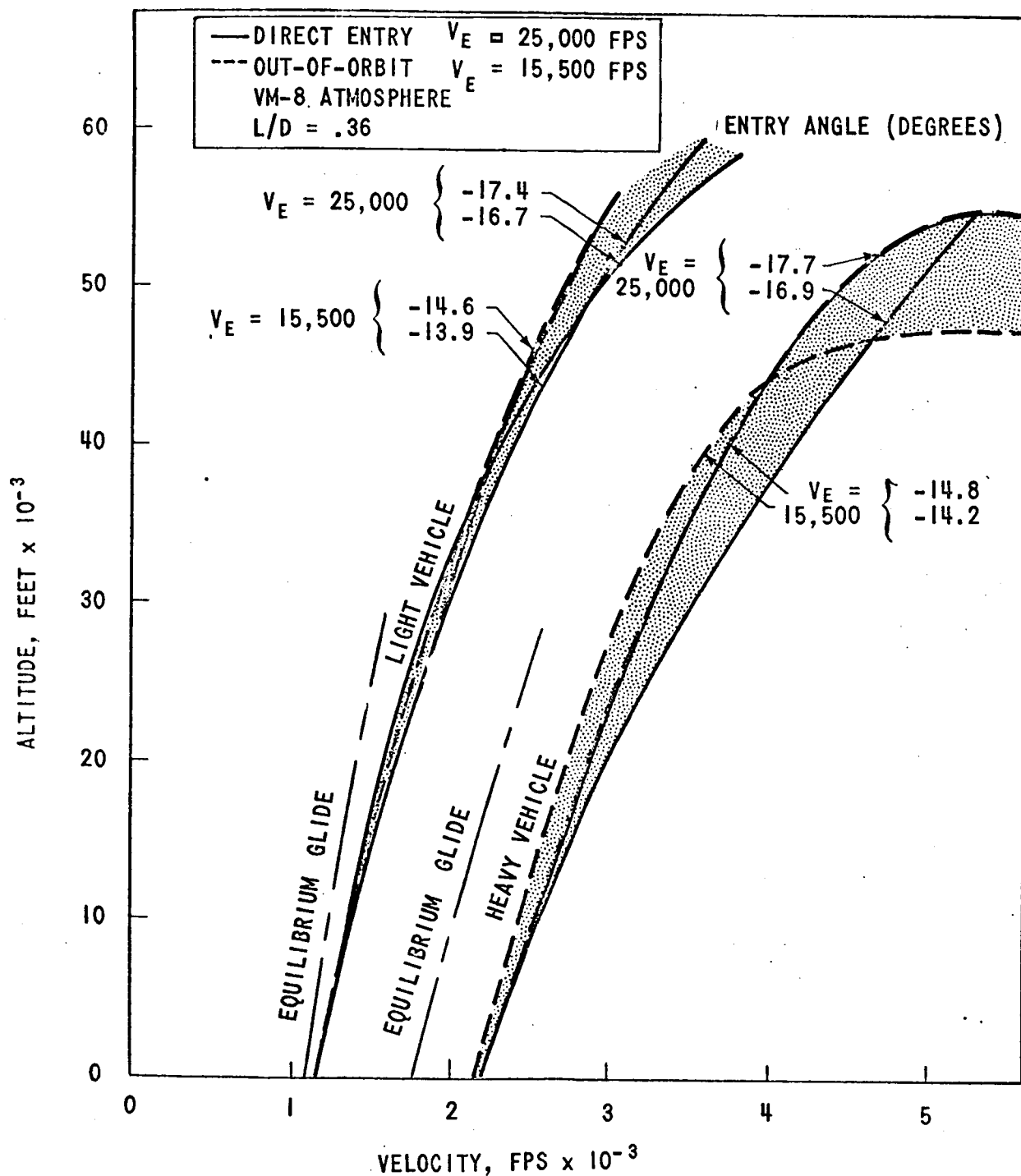


FIGURE 26 - ALTITUDE vs. VELOCITY FOLLOWING CONSTANT ALTITUDE ENTRY MANEUVER, PRIOR TO TERMINAL ROCKET IGNITION



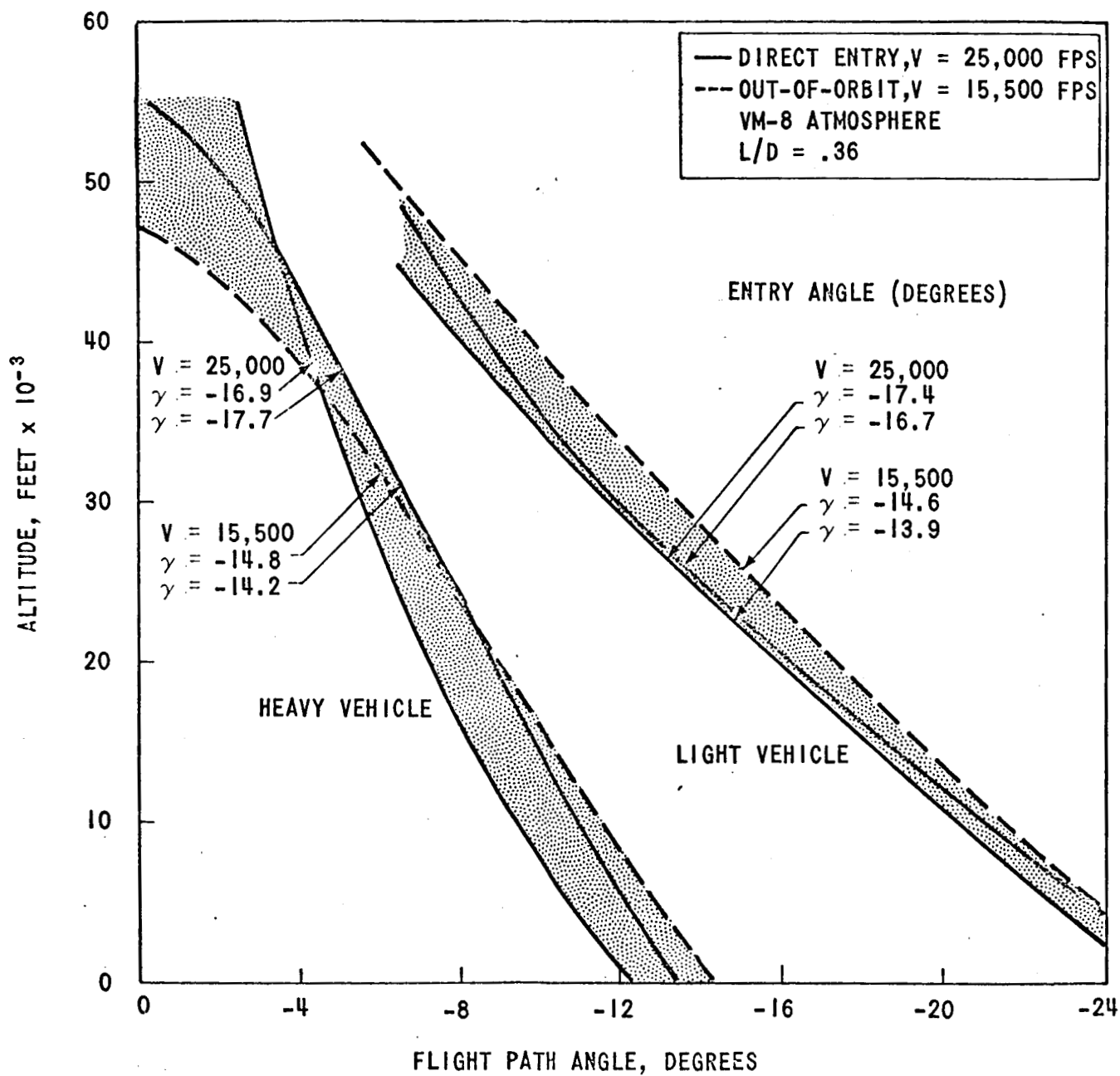


FIGURE 27 - ALTITUDE vs. FLIGHT PATH ANGLE FOLLOWING CONSTANT ALTITUDE MANEUVER, PRIOR TO TERMINAL ROCKET IGNITION

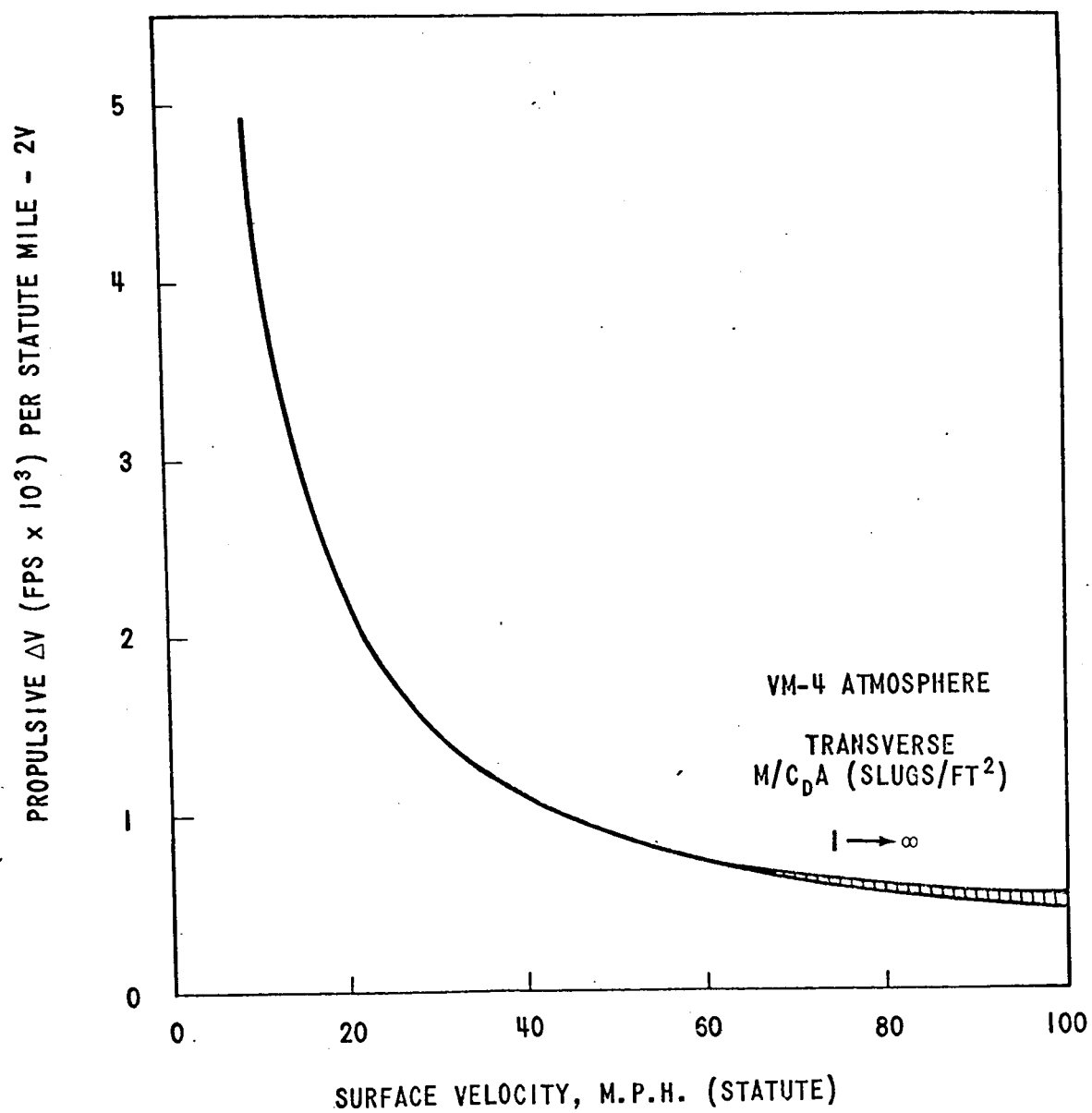


FIGURE 28 - RANGE MAKE-UP PROPULSION PENALTIES HORIZONTAL FLIGHT

## BELLCOMM, INC.

Subject: Some Considerations for the  
Atmospheric Entry of a Light  
Weight Manned Mars Landing  
Vehicle (MINIMEM) - Case 730

From: D. E. Cassidy

### DISTRIBUTION LIST

#### NASA Headquarters

Messrs. F. P. Dixon/MTY  
R. Gillespie/MTE  
E. W. Hall/MTG  
D. R. Lord/MTD  
B. G. Noblitt/MTY

#### Bellcomm, Inc.

Messrs. F. G. Allen  
G. M. Anderson  
A. P. Boysen  
R. K. Chen  
D. A. Chisholm  
C. L. Davis  
D. A. DeGraaf  
J. P. Downs  
D. R. Hagner  
P. L. Havenstein  
J. J. Hibbert  
N. W. Hinnens  
B. T. Howard  
D. B. James  
J. Kranton  
H. S. London  
K. E. Martersteck  
R. K. McFarland  
J. Z. Menard  
G. T. Orrok  
I. M. Ross  
F. N. Schmidt  
J. W. Timco  
J. M. Tschirgi  
R. L. Wagner  
J. E. Waldo  
All members Division 101  
Department 1023  
Library  
Central Files